

GERA-2758

CR-171951

# **INTERLEAVED ARRAYS ANTENNA TECHNOLOGY DEVELOPMENT**

**NASA CONTRACT NAS9-17312**

**GERA-2758**

**27 FEBRUARY 1986**

**GOODYEAR  
AEROSPACE**

(NASA-CR-171951) INTERLEAVED ARRAYS ANTENNA  
TECHNOLOGY DEVELOPMENT (Goodyear Aerospace  
Corp.) 59 E

N87-15393

CSCL 20N

Unclass  
G3/32 40244

**GOODYEAR  
AEROSPACE**

**GOODYEAR AEROSPACE CORPORATION  
*Litchfield Park, Arizona 85340-0085***

**INTERLEAVED ARRAYS ANTENNA**

**TECHNOLOGY DEVELOPMENT**

**NASA Contract NAS9-17312**

**GERA-2758  
Code 99696**

**27 February 1986**

ABSTRACT

This report covers work performed by Goodyear Aerospace Corporation for NASA-Johnson Space Center on Contract NAS9-17312 during the period 1 April 1985 through 31 January 1986. The report discusses phases one and two of a program to further develop and investigate advanced graphite epoxy waveguides, radiators, and components with application to space antennas. The objectives of these two phases were to demonstrate mechanical integrity of a small panel of radiators and parts procured under a previous contract (NAS9-16430) and to develop alternate designs and applications of the technology.

PRECEDING PAGE BLANK NOT FILMED

PRECEDING PAGE BLANK NOT FILMED

TABLE OF CONTENTS

		<u>Page</u>
ABSTRACT .....		iii
LIST OF ILLUSTRATIONS .....		vii
LIST OF TABLES .....		ix
<b>Section</b>	<b>Title</b>	
I	INTRODUCTION AND SUMMARY .....	I-1
II	ARRAY ASSEMBLY AND TEST .....	II-1
	1. General .....	II-1
	2. Adhesive Evaluation .....	II-1
	a. General .....	II-1
	b. Procedure .....	II-1
	c. Results .....	II-2
	d. Conclusion .....	II-8
	3. Joint Development .....	II-9
	a. General .....	II-9
	b. Procedures and Results .....	II-10
	c. Conclusion .....	II-15
	4. Array Assembly .....	II-15
	a. General .....	II-15
	b. L-Band Box Preparation .....	II-17
	c. Array Bonding Procedure .....	II-22
	d. Conclusion .....	II-32
	5. Environmental Testing .....	II-34
	a. Test Results .....	II-34
	b. Conclusions .....	II-35
III	PHASED ARRAY ALTERNATIVES AND PLANS .....	III-1

PRECEDING PAGE BLANK NOT FILMED

LIST OF ILLUSTRATIONS

<u>Figure</u>	<u>Title</u>	<u>Page</u>
II-1	Lap-Shear Test Specimen .....	II-4
II-2	Lap-Shear Test Specimens .....	II-6
II-3	Joint Closure Bracket .....	II-10
II-4	Waveguide Joint Specimens .....	II-12
II-5	Feed Side of X-Band Array .....	II-16
II-6	Radiator Face of X-Band Array .....	II-17
II-7	Graphite X-Band Components .....	II-18
II-8	Array and L-Band Box .....	II-19
II-9	Finished Test Module .....	II-20
II-10	L-Band Lattice Design .....	II-22
II-11	L-Band Box Layout .....	II-23
II-12	L-Band Box Construction .....	II-24
II-13	L-Band Radiator Mockup .....	II-25
II-14	Mounting Holes .....	II-25
II-15	Radiator Alignment .....	II-26
II-16	Power Divider Bonding (Three Sides) .....	II-26
II-17	Power Divider Bonding (Fourth Side) .....	II-27
II-18	Fillet Radius .....	II-27
II-19	Radiator Tack .....	II-28
II-20	Radiator Bonding .....	II-29
II-21	Faceplate Bonding (Inside Junctions) .....	II-29
II-22	Faceplate Bonding (Outer Junction) .....	II-30
II-23	Array Support Bonds .....	II-30
II-24	Syringe Extension .....	II-31
II-25	Array Support Bonds .....	II-31
II-26	Faceplate Supported Feed Option .....	II-32
II-27	Temperature-Cycled Specimens .....	II-34
II-28	Accelerometer Locations .....	II-38

LIST OF ILLUSTRATIONS (CONT)

<u>Figure</u>	<u>Title</u>	<u>Page</u>
III-1	Phased Array Elevation Plane Feed Network for One Array Panel .....	III-2
III-2	Series Feed With T/R Module .....	III-4
III-3	Generic T/R Module with Phase Shifter .....	III-5
III-4	T/R Module Development Schedule .....	III-6

LIST OF TABLES

<u>Table</u>	<u>Title</u>	<u>Page</u>
II-1	Thermoset-Adhesive Candidates .....	II-2
II-2	Lap-Shear Tensile Test Results .....	II-3
II-3	Adhesive Curing Specifications .....	II-5
II-4	Temperature Cycle Summary .....	II-36
II-5	Temperature Cycle Test Equipment List .....	II-37
II-6	Vibration Test Summary .....	II-39
II-7	Vertical Axis Resonance Search .....	II-40
II-8	Major Axis Resonance Search .....	II-41
II-9	Minor Axis Resonance Search .....	II-42
II-10	Vibration Test Equipment List .....	II-43
III-1	Module Power Output Requirements .....	III-1

## SECTION I – INTRODUCTION AND SUMMARY

This report covers work performed by Goodyear Aerospace Corporation for NASA-Johnson Space Center on Contract NAS9-17312 during the period 1 April 1985 through 31 January 1986.

The work reported on covers phases one and two of a program to further develop and investigate advanced graphite epoxy waveguides, radiators, and components with application to space antennas. This work was started on Contract NAS9-16430, and is reported in References 1 and 2.

The objectives of phases one and two were to demonstrate mechanical integrity of a small panel of radiators and parts procured under the previous contract and to develop alternate designs and applications of the technology.

Most of the emphasis was on the assembly and test of a  $5 \times 5$  element module. This effort was supported by evaluation of adhesives and waveguide joint configurations. The evaluations and final assembly considered not only mechanical performance but also producibility in large scale.

Results achieved during this contract include:

1. The  $5 \times 5$  element waveguide array was successfully assembled to precise dimensional tolerance. A preplanned assembly procedure was implemented, and production derivatives were investigated.
2. The  $5 \times 5$  array successfully passed environmental tests. Resonance characteristics of the assembly were studied.
3. Failure modes of the silver coating and of adhesives were studied during adhesive evaluation. Four thermoset adhesives were selected for joint and array assembly.
4. Several waveguide joint designs were built and evaluated with respect to tooling, labor, and performance. A simple fillet joint was selected for assembly of the  $5 \times 5$  array.

In addition to the foregoing, a small effort on incorporation of distributed transmit/receive (T/R) modules was undertaken. Only preliminary information was developed prior to deletion of the task by agreement between Goodyear Aerospace and NASA.

REFERENCES

1. "Shaped Reflector/Multiple Horn/Interleaved Array Antenna Technology Development," GERA-2644, Goodyear Aerospace Corporation, Litchfield Park, AZ, 30 June 1983.
2. "Interleaved Array Antenna Technology Development," GERA-2702, Goodyear Aerospace Corporation, Litchfield Park, AZ, 30 January 1985.
3. "Technical Briefing, Interleaved Arrays Antenna Technology Development, Phase One," GIB-9668, Goodyear Aerospace Corporation, Litchfield Park, AZ, 20 August 1985.

## SECTION II – ARRAY ASSEMBLY AND TEST

### 1. GENERAL

A 5 x 5 graphite/epoxy X-band waveguide array was built and environmentally tested to prove the feasibility of the mechanical design and high volume assembly techniques. Prior to assembly of the array, work was done to develop joint designs and techniques which might be easily adapted to production. The following paragraphs describe in detail the adhesive evaluation, the joint configuration development, the array assembly procedure, and environmental testing done on the final product.

### 2. ADHESIVE EVALUATION

#### a. General

Samples of eight brands of silver-filled conductive adhesives were collected for mechanical evaluation. All eight candidates evaluated were thermoset adhesives. A lap-shear test was conducted to show the relative strengths of samples as well as to establish quantitative shear strength for the bracketed joint design. The adhesives tested are listed with their physical properties in Table II-1, and with the test results in Table II-2.

#### b. Procedure

The objective of the test procedure was to model, as closely as possible, the design configuration and assembly processes anticipated in a production environment. The samples were tested on silver-plated graphite substrates that were hand-assembled and cured per manufacturer instructions.

Silver-plated graphite tape test coupons were sawed into lap-shear plates as described in Figure II-1. Two coupons were used in this way, one with a smooth silver-side texture and the other with a rough, severely etched silver-side finish. Some of the graphite fiber, loosened in the severe etch, was removed during cleaning. The silver plating coverage remained complete. Sixteen specimens, two of each adhesive, were assembled and tested. To help establish preferred substrate surface conditions, one specimen of each adhesive sample bonded smooth surface plates, while the other was used on rough textured plates.

TABLE II-1 - THERMOSET ADHESIVE CANDIDATES

Adhesive Type	Maximum Service Temperature (Deg F (Deg C))	Minimum Service Temperature (Deg F (Deg C))	Volume Resistivity (Ohm-cm)	Coefficient of Thermal Expansion (ppm/Deg F (Deg C))	Components	Cure Temperature (Deg F)	Published Lap-Shear Strength (psi)	Measured Lap-Shear Strength (psi)	Matrix
Transcene PDA S-500	700 (375)	-49 (-45)	$1 \times 10^{-4}$		1	518	2000	349	Polyimide
Transcene Microcircuit Type-N	390 (200)	-76 (-60)	$2 \times 10^{-3}$	50 (90)	1	275-350	3500	824	Epoxy
Transcene Silver Bond Type-40	390 (200)	-85 (-65)	$1 \times 10^{-4}$		2	120-300	1500	883	Epoxy
Ablestik 34-1 LM1 T	300 (150)	-67 (-55)	$2 \times 10^{-4}$	30 (55)	1	250-320	1600	658	Epoxy
Amicon C-770			$1 \times 10^{-3}$		1	250-430	1500	85	Epoxy
Emerson & Cuming Ecco Bond 83C	275 (135)	-65 (-54)	$4 \times 10^{-4}$	25 (45)	2	RT-220*	1000	781	Epoxy
Emerson & Cuming Ecco Bond 56C	350 (177)	-70 (-57)	$2 \times 10^{-4}$	20	2	150-200	800	874	Epoxy
Emerson & Cuming Ecco Bond 59C	500 (260)	-80 (-62)	$1 \times 10^{-3}$	35 (63)	1	RT-300	300	194	Silicone

\*Room temperature.

A thin layer of adhesive was spread on the bond surface of each plate. The plates were pressed together with light finger pressure. Excess adhesive was allowed to flow out. The cure schedules are listed in Table II-3. The cured specimens were pulled to failure on an Instron tensile tester.

### C. Results

The broken test specimens are displayed in Figure II-2 (2 sheets) to illustrate the failure features on the bonding surface. The nine specimens showing the highest lap-shear strength failed at the silver coating-to-graphite interface and were not failures of the adhesives.

In these cases the strength of the bonding agents exceeded the adhesion strength of the silver to the graphite. Three of the adhesives demonstrated failure predominantly within the adhesive material (cohesive mode of failure), as opposed to failure at the adhesive/silver interface (adhesive mode of failure). These failures occurred at stresses well below the adhesion strength of the silver coating and were therefore

TABLE II-2 — LAP-SHEAR TENSILE TEST RESULTS

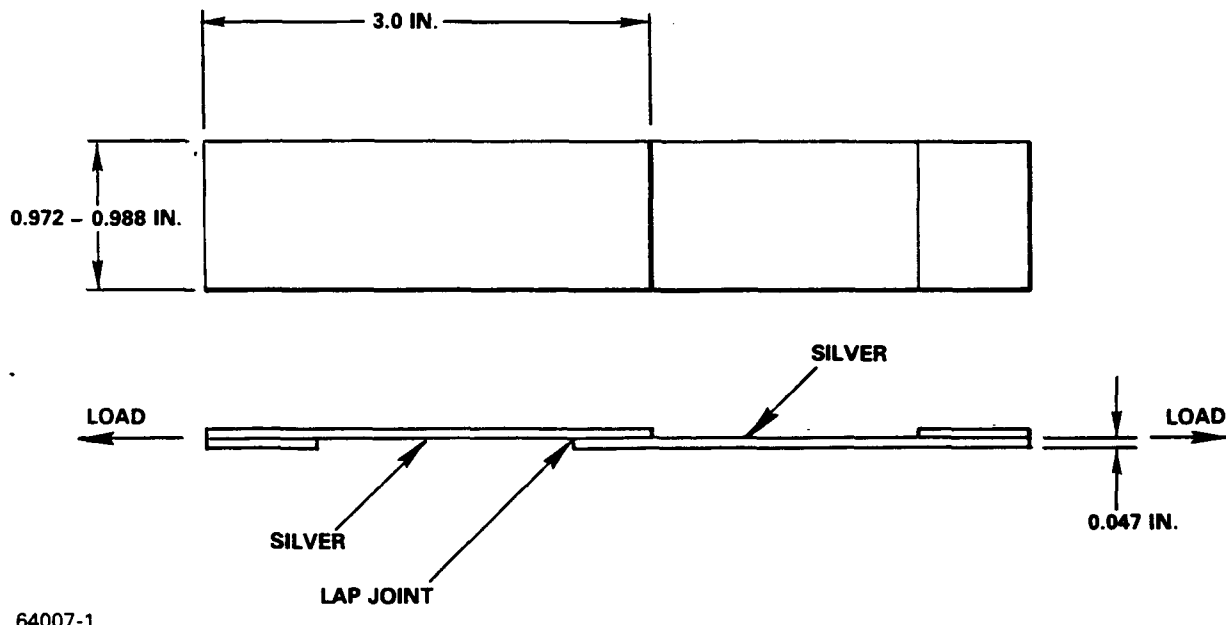
Adhesive	Specimen (No.)	Ultimate Stress (psi)	Average	Failure Mode	Plate Surface
PDS-S-500	1	340	349	Adhesive (Ag)*	Rough Smooth
	2	358		Adhesive (Ag)	
Microcircuit Type-N	3	934	824	Mostly adhesive (Ag)	Rough Smooth
	4	715		Adhesive (Ag)	
Silver Bond Type-40	5	960	883	Adhesive (Ag)	Rough Smooth
	6	806		Adhesive (Ag)	
Ablestik 84-1 LMI T	7	454	658	Mostly cohesive	Rough Smooth
	8	862		Mostly adhesive (Ag)	
Amicon C-770	9	122	85	Cohesive	Rough Smooth
	10	48		Cohesive	
Ecco Bond 83C	11	851	781	Adhesive (Ag)	Rough Smooth
	12	712		Adhesive (Ag)	
Ecco Bond 56C	13	709	874	Mostly mixed	Rough Rough
	14	1038		Mostly mixed	
Ecco Bond 59C	15	156	194	Cohesive	Rough Rough
	16	233		Mostly cohesive	

\*Ag = silver.

unacceptable. Very little evidence was found of failure by loss of adhesion at the adhesive/silver interface.

Of the specimens exhibiting a predominantly adhesive mode of failure, those with rough severely etched substrates demonstrated a high lap-shear strength.

The more subjective ease of application differences between adhesives were minor. One-part adhesives were, of course, simpler to prepare and less vulnerable to mistakes. Three of the four strongest adhesives were two-part adhesives.



64007-1

Figure II-1 — Lap-Shear Test Specimen

Adhesive viscosity varied widely. Ecco Bond 56C was the most viscous and therefore the most difficult to spread evenly on the substrate. Ablestik 84-1 LMI T was the least viscous and easiest to spread. The following comments apply to the individual adhesive samples:

**PDA-S-500:** Adhesive failure of the silver coating at the points of contact. More than half the bonding area was void of adhesive, which accounts for the poor performance of the specimens. High viscosity, premature curing, or inadequate pressure could be reasons for the poor bond coverage.  
Unsatisfactory.

**Microcircuit Type-N:** Adhesive failure of silver coating over at least 80 percent of the bond surface. Satisfactory.

**Silver Bond Type-40:** Adhesive failure of silver coating over entire bond surface. Satisfactory.

**Ablestik 84-1 LMIT:** Cohesive failure of one specimen. Unsatisfactory.

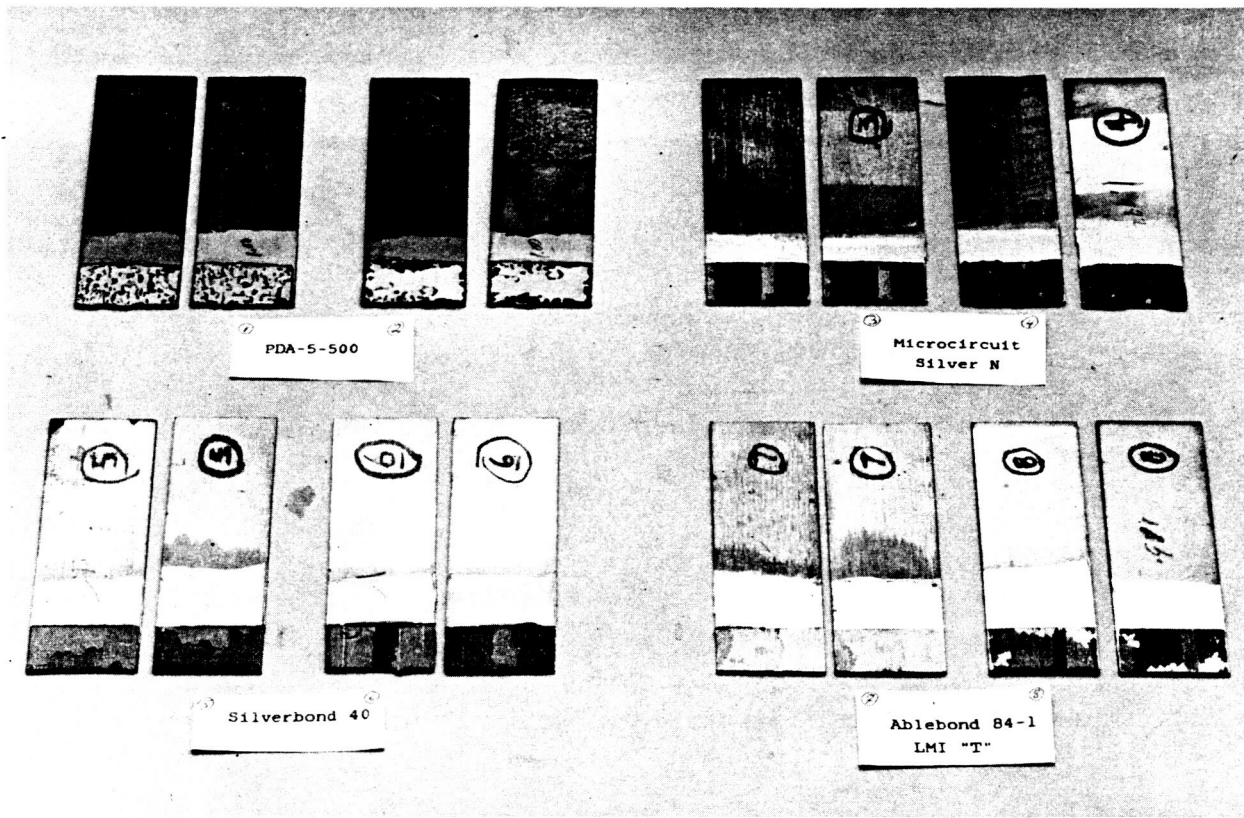
**Amicon C-770:** Cohesive failure of both specimens. Unsatisfactory.

TABLE II-3 – ADHESIVE CURING SPECIFICATIONS

Adhesive	Cure Schedule (Deg C)	Comments
Transcene PDA-S-500	150* for 15 minutes plus 270 for 30 minutes	One part
Micrcircuit Silver Type-N	135 for 5 hours, or 150* for 1-1/2 hours, or 175 for 30 minutes	One part
Transcene Silver Bond Type-40	100* for 2 hours	Two-part epoxy. 100:3.6, A:B
Ablestik 84-1 LMI T	125 for 2 hours, or 150* for 1 hour, or 160 for 1/2 hour	One-part epoxy. Spreads easily
Amicon C-770	125 for 1 hour 150* for 30 minutes 250 for 1 minute	One-part epoxy
Ecco Bond 56C With Catalyst 11	77 for 8 hours, or 121* for 1 hour	30:1, or 1-1/2 drops catalyst to 1 gm 56C. Poor spreadability
With Catalyst 9	49 for 2 hours 65C-93C for a few minutes	40:1 by weight, or 1 drop catalyst to 1 gm 56C  Add 10-percent toluene (maximum) if needed for thinner
Ecco Bond 59C Catalyst 59	149* for 6 hours	2-percent catalyst by weight
Ecco Bond 83C Catalyst 9	65* for 1 hour	2.7-percent catalyst by weight. Unusually slow cure

\*Schedule used for test specimens.

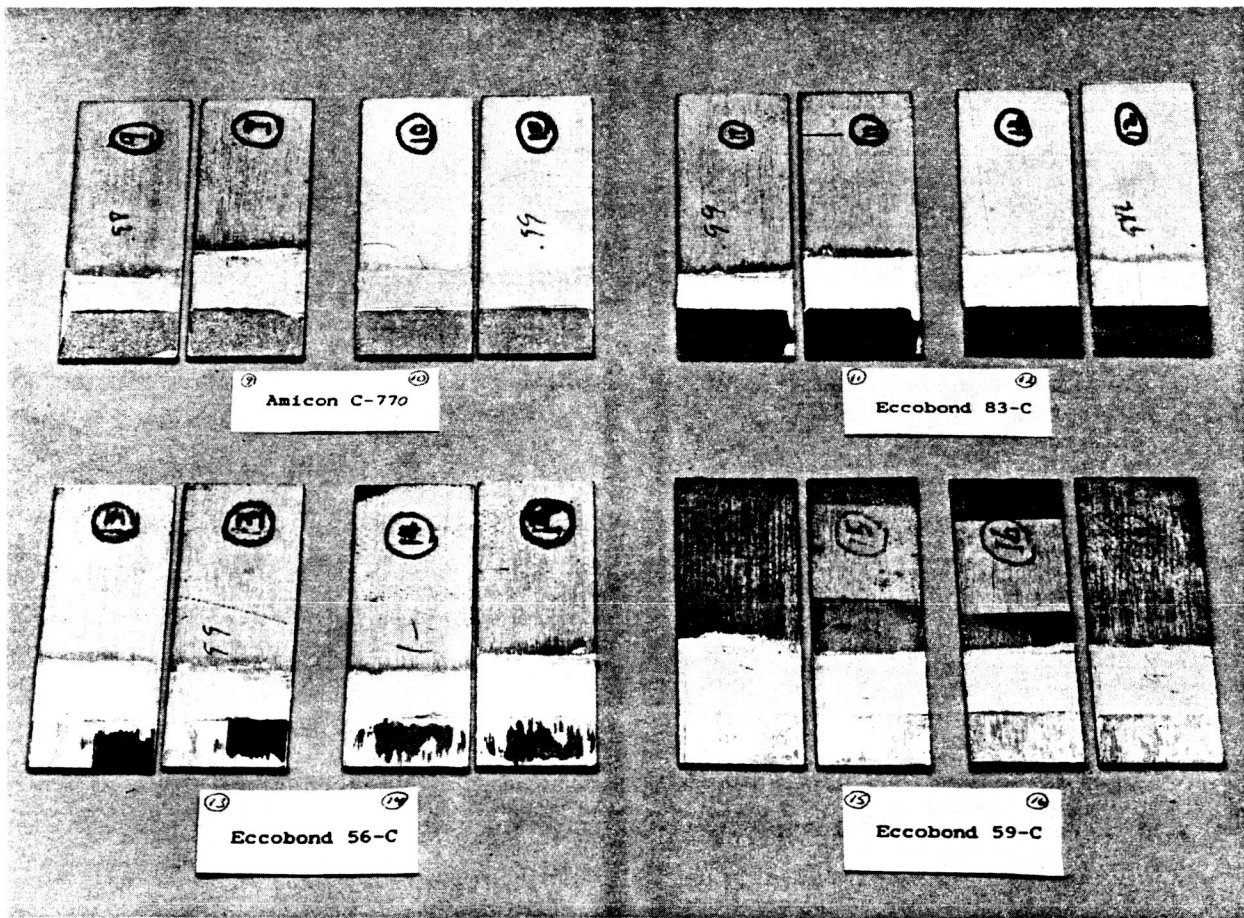
ORIGINAL PAGE IS  
OF POOR QUALITY



G860116 02

Figure II-2 – Lap-Shear Test Specimens (Sheet 1 of 2)

ORIGINAL PAGE IS  
OF POOR QUALITY



G860116 01

Figure II-2 – Lap-Shear Test Specimens (Sheet 2 of 2)

Ecco Bond 83C: Adhesive failure of silver coating over entire surface. Satisfactory.

Ecco Bond 56C: Adhesive failure of the silver coating over about half the bond surface of both specimens. Significant cohesive failure over remaining area. Some evidence of voids and adhesive failure of adhesive/silver interface. Graphite fractured on one specimen. These specimens showed the best silver-to-graphite adhesion in light of the fractured graphite, cohesive failure, and good performance. The adhesive appears to be near its limits in spite of good performance. Satisfactory.

Ecco Bond 59C: Mostly cohesive failure except for some adhesive failure of the adhesive. Unsatisfactory in strength, but may be useful if flexural toughness is required.

d. Conclusion

Lap-shear strength of four of the eight adhesives tested exceeded the adhesion of the silver-to-graphite substrate and therefore could not be determined. All of these adhesives – Transcene Microcircuit Type-N, Transcene Silver Bond Type-40, Emerson & Cuming Ecco Bond 83C, and Emerson & Cuming Ecco Bond 56C – are satisfactory for assembly of the mechanical test array. Ecco Bond 83C was chosen for evaluation in the joint development phase of the program because of its low coefficient of thermal expansion, ease of application and cure, and availability.

All the adhesives have similar published values for minimum service temperature and resistivity. Some of the joints built with Ecco Bond 83C were thermal cycled down to 80 deg F as described in Environmental Testing, paragraph II.5. The higher maximum service temperatures available with the polyimide PDA-S-500 and the silicone Ecco Bond 59C will not be required for a space antenna.

Any improvements in strength of bonded joints must focus on the weakest link in the bond, adhesion of silver to the graphite/epoxy substrate. Until better metal adhesion is developed, the full strength of the bonding adhesive cannot be utilized.

Improved metal adhesion to the rough severely etched substrates will be evaluated

with respect to electrical behavior of this surface condition. It appears that increased surface roughness appreciably degrades electrical performance of the 18-in. electrical test waveguide tubes.

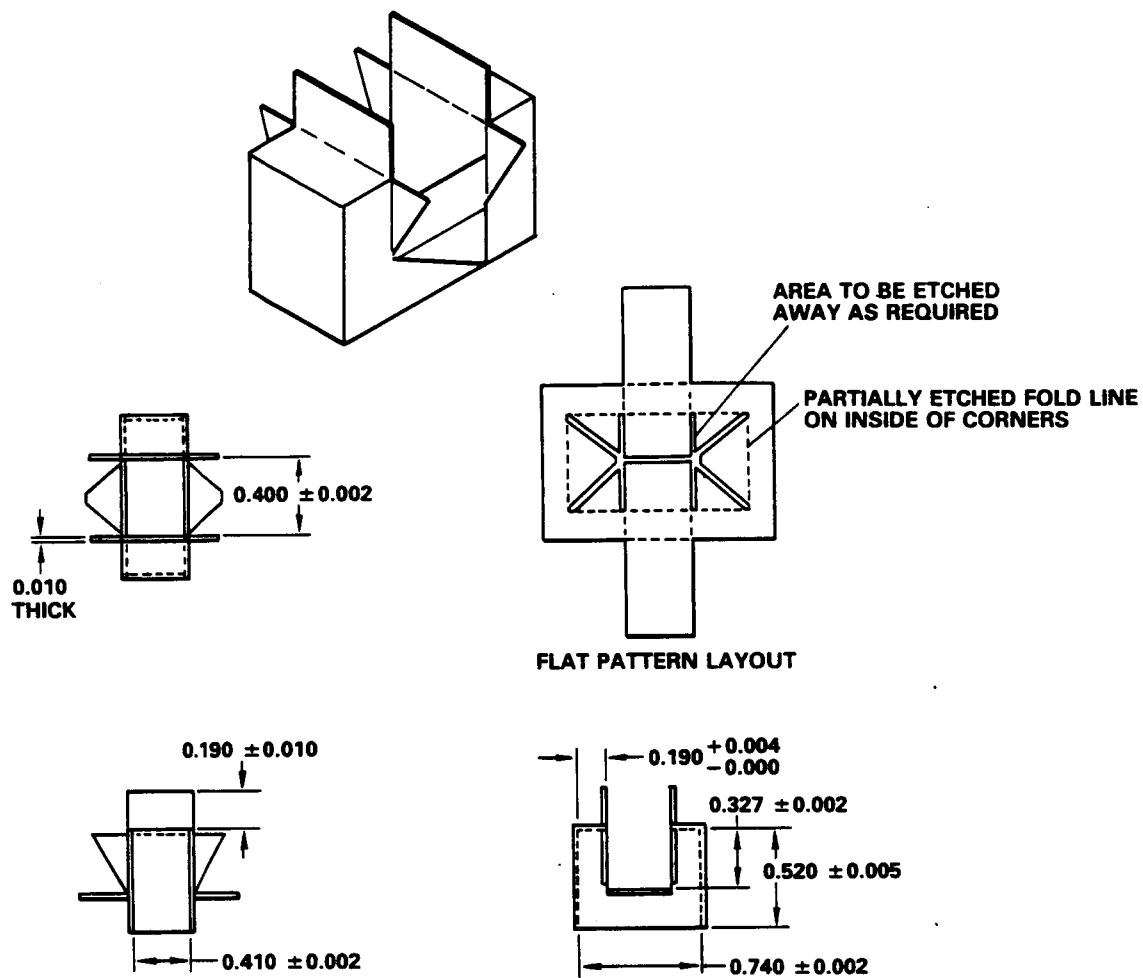
A joint design that overcomes the inadequacies of the silver adhesion involves the addition of a sleeve or bracket. A bracket can be used to increase the surface area available for bonding and/or extend the bond surface past the metallized portion of the waveguide to bond directly on the graphite/epoxy substrate. Such radiator joint brackets have been developed for joint assembly and closure. The brackets are chemically milled (subtractive etch) from 0.010-in.-thick sheets of 1/4 hard stainless steel 300 or 1/2 hard brass. The brackets are hand folded at half depth, one side only, etch lines to obtain the box structure shown in Figure II-3. The cut lines and fold lines are located using CAD-generated photo-reduced artwork. This technique is well suited to high-volume production of precision parts such as the radiator joint closure bracket or other closure and assembly hardware. The brackets and adhesive-only joints were built and evaluated as described in the following paragraphs.

### 3. JOINT DEVELOPMENT

#### a. General

Configurations and fabrication techniques of graphite waveguide joints were studied prior to assembly of the 5 x 5 mechanical test array. An appropriate joint design was selected for use on the 5 x 5 array, and several new ideas evolved for future consideration.

Four thermoset conductive adhesives were found acceptable in phase one. All four met or exceeded the adhesion strength of the silver-plated coating to the graphite substrate. Each published acceptable electrical conductivity and similar service temperature ranges. Ecco Bond 83C was used in the thermoset joint configurations because of its availability and ease of application. Also evaluated was Amicon C-933-45 one-part conductive thermoplastic adhesive and 60 Sn/40 Pb solder. All evaluations were subjective. No quantitative data was measured on the test joints.



NOTES:  
MATERIAL TO BE BRASS, 1/2 HARD 0.010-IN. THICK  
DIMENSIONS IN INCHES

64007-2

Figure II-3 – Joint Closure Bracket

b. Procedures and Results

Joints were constructed from the electrical evaluation waveguides purchased during phase one. Small test pieces were machined from the waveguides to model the feeder-to-radiator joints in the 5 x 5 array.

The joint configuration selected for the 5 x 5 array is a simple fillet of thermoset adhesive applied by hypodermic needle. The joint was neat in appearance and

strong. A steady, meticulous hand is required for a clean continuous fillet, necessitating the use of skilled labor.

The bracketed joint described in Figure II-3 was further developed but did not prove convenient with either thermoset or thermoplastic adhesives. The thermoplastic adhesive did not provide acceptable bond strength without pressure. High-volume production of thermoplastic-bonded bracket joints with adequate tooling may have advantages over the thermoset joints, but the necessary clamping tools were too expensive for this application. The vapor phase soldered joint also showed promise and should be investigated in future studies.

The following comments describe the various test joints, approximately in their chronological order:

Group 1

A. Hot melt glue with bracket.

**Procedure:** Master Mechanics hot melt glue was tested as representative of a thermoplastic adhesive. The glue was heated and brushed on both waveguide pieces and the unbent bracket with an acid brush. The pieces were assembled with the bracket, with the bracket tension holding the three pieces in alignment. The assembly was reheated to reflow the glue. A heat gun was used as a heat source.

**Analysis:** The resultant assembly was neat and strong, but not conductive. This test led to the testing of a conductive thermoplastic adhesive, Amicon C-933-45.

B. Ecco Bond 83C with bracket.

**Procedure:** Wet 83C adhesive was smeared on both waveguide pieces and on the inside of the bracket and the pieces pressed together. Excess adhesive was laboriously removed with swabs and tissue paper.

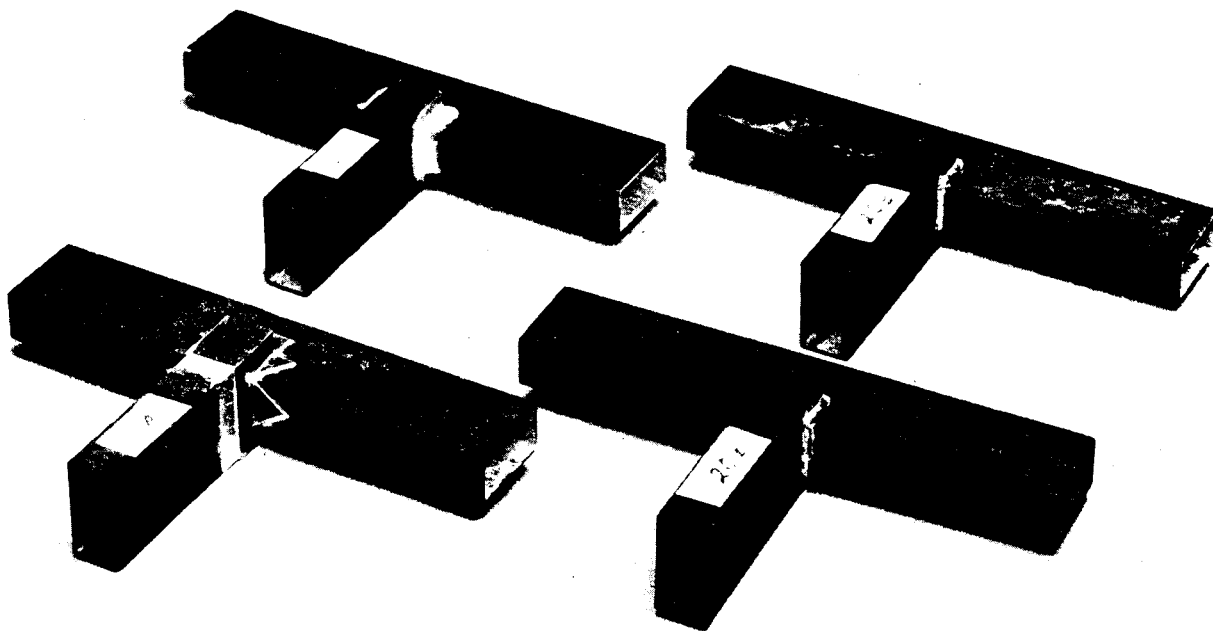
**Analysis:** Assembly was strong and the outward appearance good because of the time spent removing the excess squeeze-out. Time thus

spent makes this technique impractical for large-scale production. Also, a large and undesirable squeeze-out of glue was observed inside the radiator in the vicinity of the coupling slot.

C. Ecco Bond 83C without bracket.

**Procedure:** The waveguide pairs were assembled dry with no bracket. Ecco Bond 83C was applied in copious amounts, then smoothed into large fillets and the excess removed with swabs and tissue paper.

**Analysis:** Assembly was strong with no glue squeeze-out on the inside. Considerable time was spent dressing the fillet. A finished specimen is shown labeled 1C in Figure II-4.



G960213 37

Figure II-4 – Waveguide Joint Specimens

D. 60/40 solder T-joint.

**Procedure:** Two 1-in. x 2-in. flat pieces cut from spare tape test coupons were soldered at a right angle using a soldering iron.

**Analysis:** Overall appearance was good with evident high strength.

However, the application of solder was judged to be too difficult for use in the 5 x 5 array.

E. 60/40 solder lap joint.

**Procedure:** Two 1-in. x 2-in. pieces were tinned prior to the actual lap joint soldering using a propane torch and acid brush to spread the solder.

**Analysis:** The heat output from the torch has hard to control, and the silver plating burned from the graphite in spots. This approach may be workable with more closely controlled heat application such as vapor phase soldering.

F. Vapor phase solder T-joint.

**Procedure:** Two 1-in. X 2-in. pieces were fixed at a right angle to each other with a solder wire set against the corner. The assembly was placed in a vapor phase solder reflow chamber at 410 deg F for 1 minute, then allowed to dwell at 130 deg F for 1.5 minutes.

**Analysis:** The solder wicked well into the corner and produced a bond strong enough to peel the silver off the graphite. Poor silver adhesion may have been caused by the soldering process, or may have already existed in the specimen. Further study of a vapor phase solder joint is recommended using solder paste or solder preforms.

Group 2

A. Thermoplastic with bracket.

**Procedure:** The Amicon C-933-45 was thinned to a spreadable consistency with the recommended thinner (cellosolve acetate) and painted on the waveguide pieces and unbent bracket. Adhesive thickness (dried) was 0.002 to 0.003 in. The pieces were assembled with bracket tension only

holding the assembly together and heated to the reflow temperature. The manufacturer recommends a clamping pressure of 10-25 psi during reflow. Pressure could not be applied to all bond surfaces without elaborate tooling. The Master Mechanics thermoplastic of Method A, Group 1 worked well without clamping.

Analysis: Adhesion was very poor. This performance may be attributed to inadequate clamping pressure.

B. Ecco Bond 83C with syringe, no bracket.

Procedure: Ecco Bond 83C was spread on the mating surfaces of the waveguide. The waveguide was held together with rubber bands, and fillets of 83C adhesive applied on the outside with a syringe. The syringe had a 0.047-in.-diameter orifice.

Analysis: Bond was strong, and appearance was acceptable. Some glue squeeze-out was noted inside the guide, as expected.

C. Ecco Bond 83C with syringe, no bracket.

Procedure: No glue was spread on mating surfaces of the waveguide. The waveguide pieces were held in alignment with rubber bands, and fillets of glue were run around the junctions. No glue was put on mating surfaces.

Analysis: Assembly was strong with neat appearance and no glue squeezed out on the inside. Two specimens are shown labeled 2C I and 2C II in Figure II-4.

Group 3

A. Ecco Bond 83C with bracket and polyglycol.

Procedure: The hollow waveguide tubes were filled with a wax polyglycol, for support during machining. The polyglycol was left in the tubes to limit internal spillover. Ecco Bond 83C was spread on the machined waveguide pieces and inside the bracket, the bracket pushed into place, and the excess removed with swabs and tissue paper. This subassembly was allowed to cure. Then the mating surfaces of the waveguide and of

the other waveguide were brushed with 83C adhesive, pressed together, and the excess glue removed with swabs and tissue paper. The 83C adhesive was allowed to cure. Then the assembly was soaked in hot water to remove the polyglycol.

**Analysis:** Glue squeeze-out completely covered the coupling slot area, but was of a uniform thickness because of the polyglycol. This assembly was the most time consuming of any because of the additional steps and the cleanup of glue squeeze-out around the bracket. The assembly was very strong. A specimen is shown labeled 3A in Figure II-4.

**B. Ecco Bond 83C with polyglycol, without bracket.**

**Procedure:** Ecco Bond 83C was spread on mating waveguide surfaces, the waveguide pressed together and held with rubber bands, and fillets of 83C adhesive applied to the outside corner with a syringe. After the 83C adhesive cured, the polyglycol was melted out by soaking the assembly in hot water.

**Analysis:** Assembly was strong and acceptable in appearance, but substantial glue squeeze-out was noted around the coupling slot area. The squeeze-out was flattened because of the polyglycol.

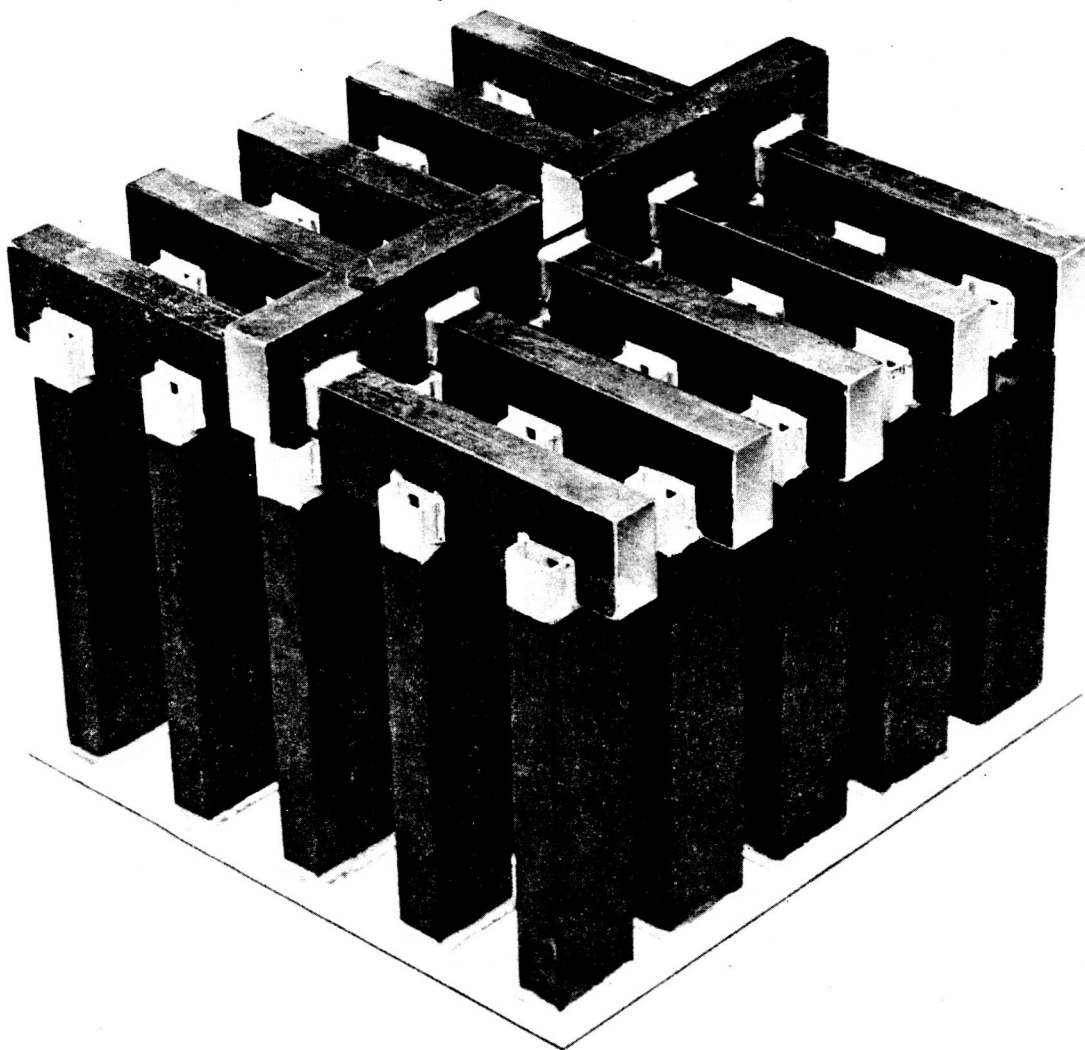
**C. Conclusion**

The most acceptable joint was the syringe-applied fillet joint of Group 2, Method C. This method was used on the radiator joints of the 5 x 5 array. Electrical function of this joint requires the bonding of a rectangular closure tab across the open shoulders of the radiator element.

**4. ARRAY ASSEMBLY**

**a. General**

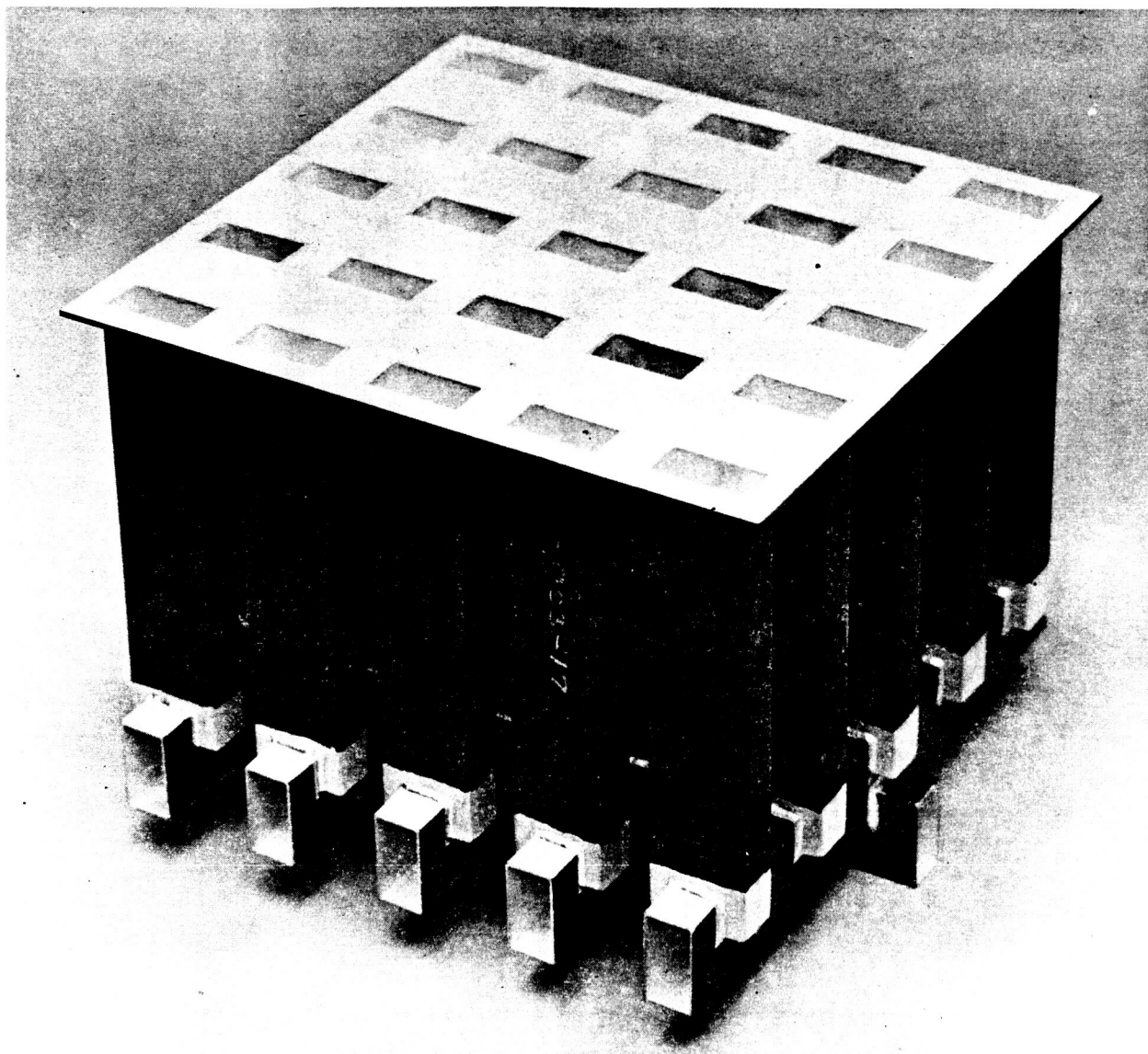
The 5 x 5 graphite/epoxy X-band waveguide array was assembled upon positive evaluation of four thermoset adhesives and selection of the syringe fillet joint as the preferred joint configuration. The array shown in Figures II-5 and II-6 was built from silver-coated graphite/epoxy fabricated on the previous contract. Some components, a faceplate, two power dividers, and two radiators are pictured in Figure II-7.



G851014 28

Figure II-5 – Feed Side of X-Band Array

The array was designed to be supported during environmental test by a graphite structure mechanically similar to the L-band lattice of the interleaved arrays antenna design. Figure II-8 illustrates the insertion of the array into the L-band box structure to form the completed test module of Figure II-9 (2 sheets). The  $5 \times 5$  array of Figure II-5 has a mass of 196 grams. The complete assembly, including the L-band box, has a mass of 709 grams.



G851014 30

Figure II-6 – Radiator Face of X-Band Array

The following paragraphs describe the array assembly processes in detail.

**b. L-Band Box Preparation**

The array's mechanical interface structure, referred to herein as the L-band box, is similar to an interleaved L-band lattice structure inasmuch as both incorporate broad, thin-walled cavities to be used as L-band radiators, and both support the

ORIGINAL PAGE IS  
OF POOR QUALITY

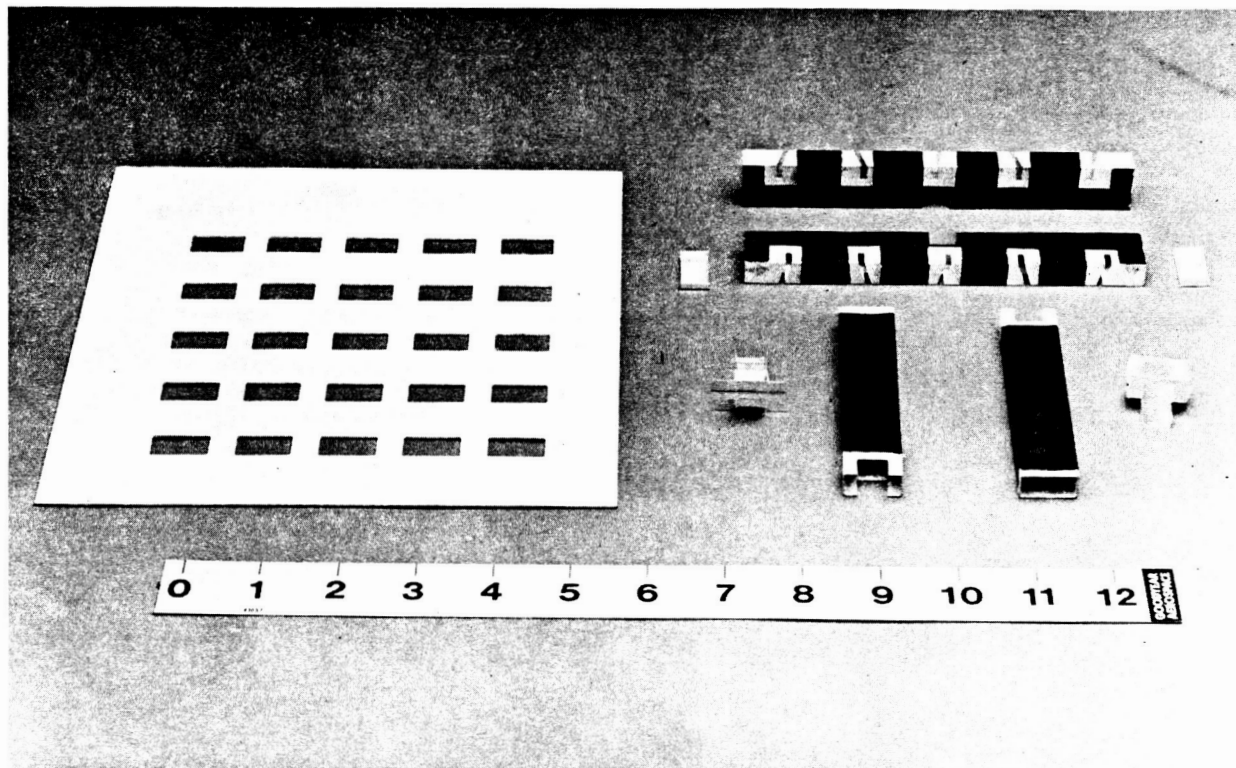
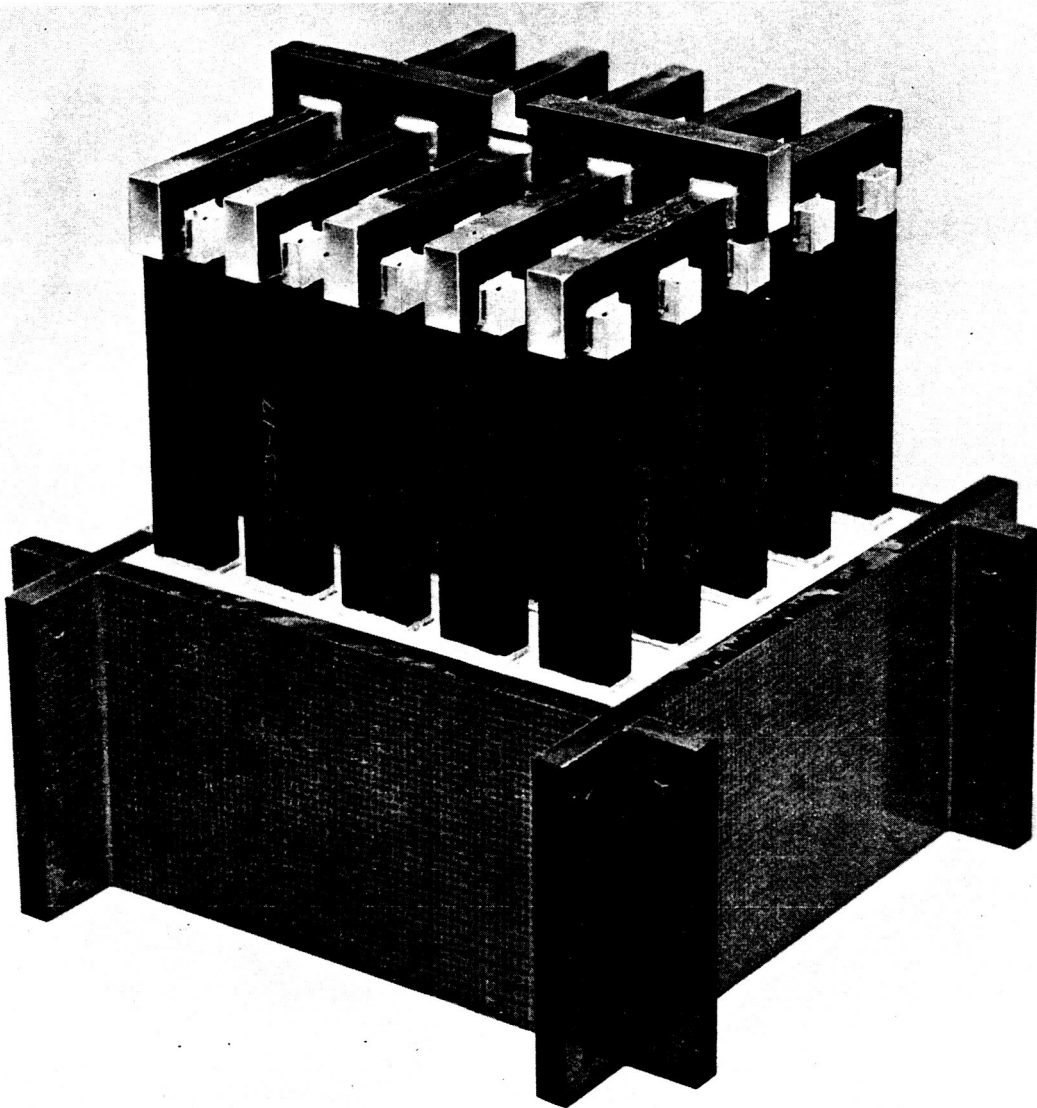


Figure II-7 – Graphite X-Band Components

X-band assembly at the faceplate and secondary power dividers. Differences between this box and the lattice design include exact dimensions and, more important, construction. The final lattice design, Figure II-10, will be a precision unidirectional tape structure that minimizes the effects of Z-direction expansion. The L-band box is not as thermal-expansion controlled as the lattice or the X-band array because of its time-expedient laminated fabric construction. Therefore, only joint specimens were temperature cycled. Mechanical loading of the box by the X-band array is identical to that for the interleaved lattice design.

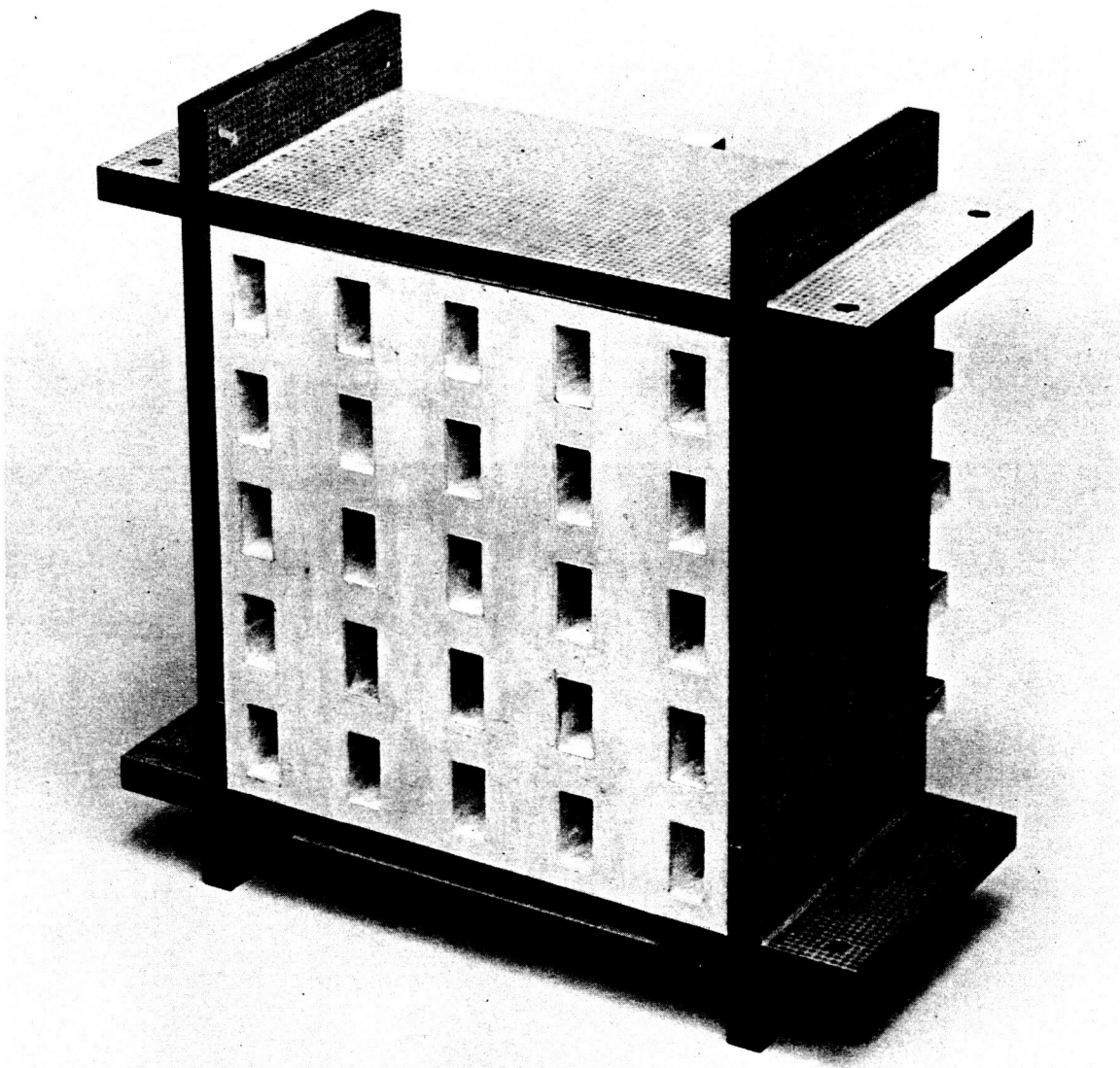


G851014 29

Figure II-8 – Array and L-Band Box

L-band box internal dimensions were selected at 5.400 in. x 5.772 in. to place the end of the secondary power dividers over the center of the box walls and to have the box walls equidistant from the radiators on all four sides (Figure II-11).

ORIGINAL PAGE IS  
OF POOR QUALITY

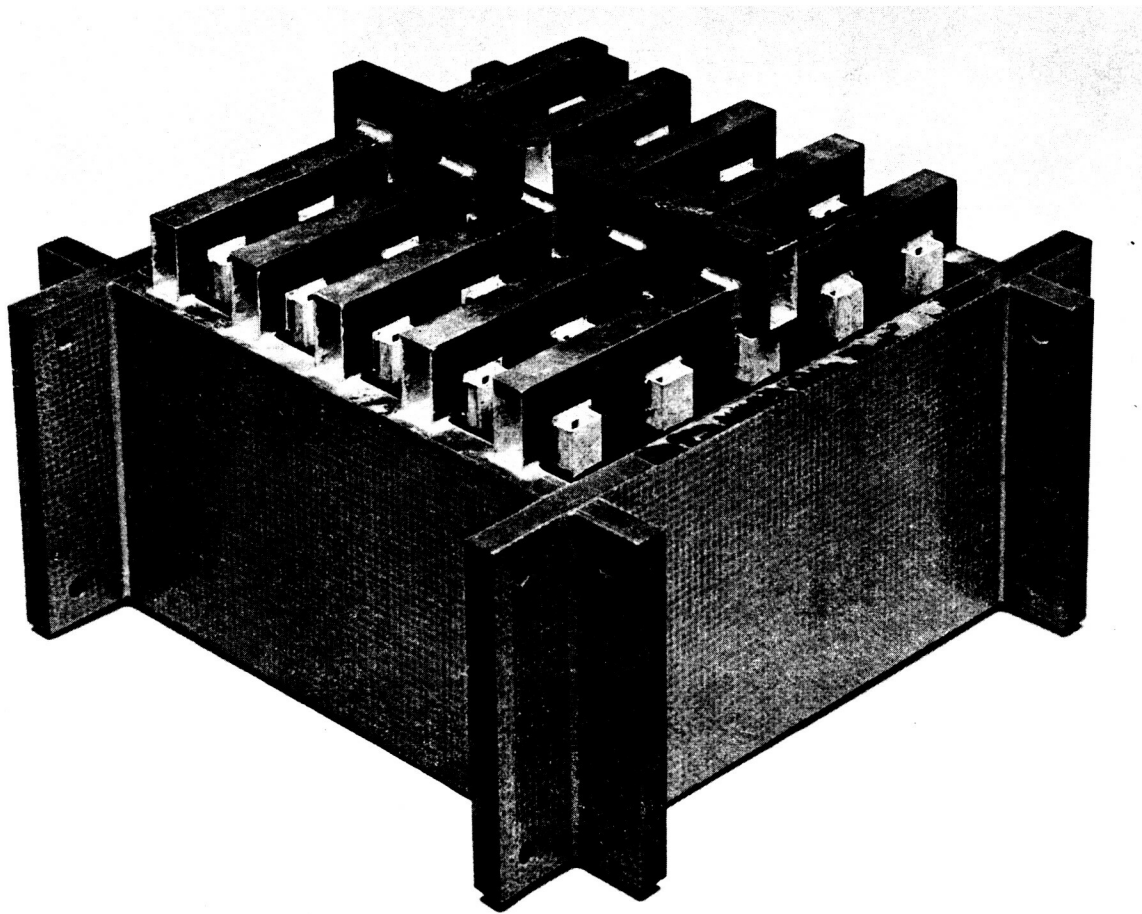


G851021 01

Figure II-9 – Finished Test Module (Sheet 1 of 2)

Slots were cut into the four pieces that enabled them to be assembled into a box-shaped structure (Figure II-12). Carbide tooling used to machine the slots was rapidly dulled. Diamond-tipped cutters are recommended for graphite machine work.

The open ends of the L-band radiators toward the rear (feed end) of the antenna were plugged with pieces of laminated graphite made from graphite waveguide



G860213 35

Figure II-9 – Finished Test Module (Sheet 2 of 2)

scraps and EA934 adhesive. Unfortunately, the grain structure of the plugs did not match the grain structure of the L-band pieces in one direction (Figure II-13). Mounting holes were drilled in the edges on 7.25-in. x 2.75-in. centers for no. 10 screws (Figure II-14).

The box pieces were then bonded into one structure with EA934 adhesive. The box was assembled on a flat surface using one of the faceplates to assure orthogonality. The finished box was sanded lightly on a surface plate to true up the edge surfaces.

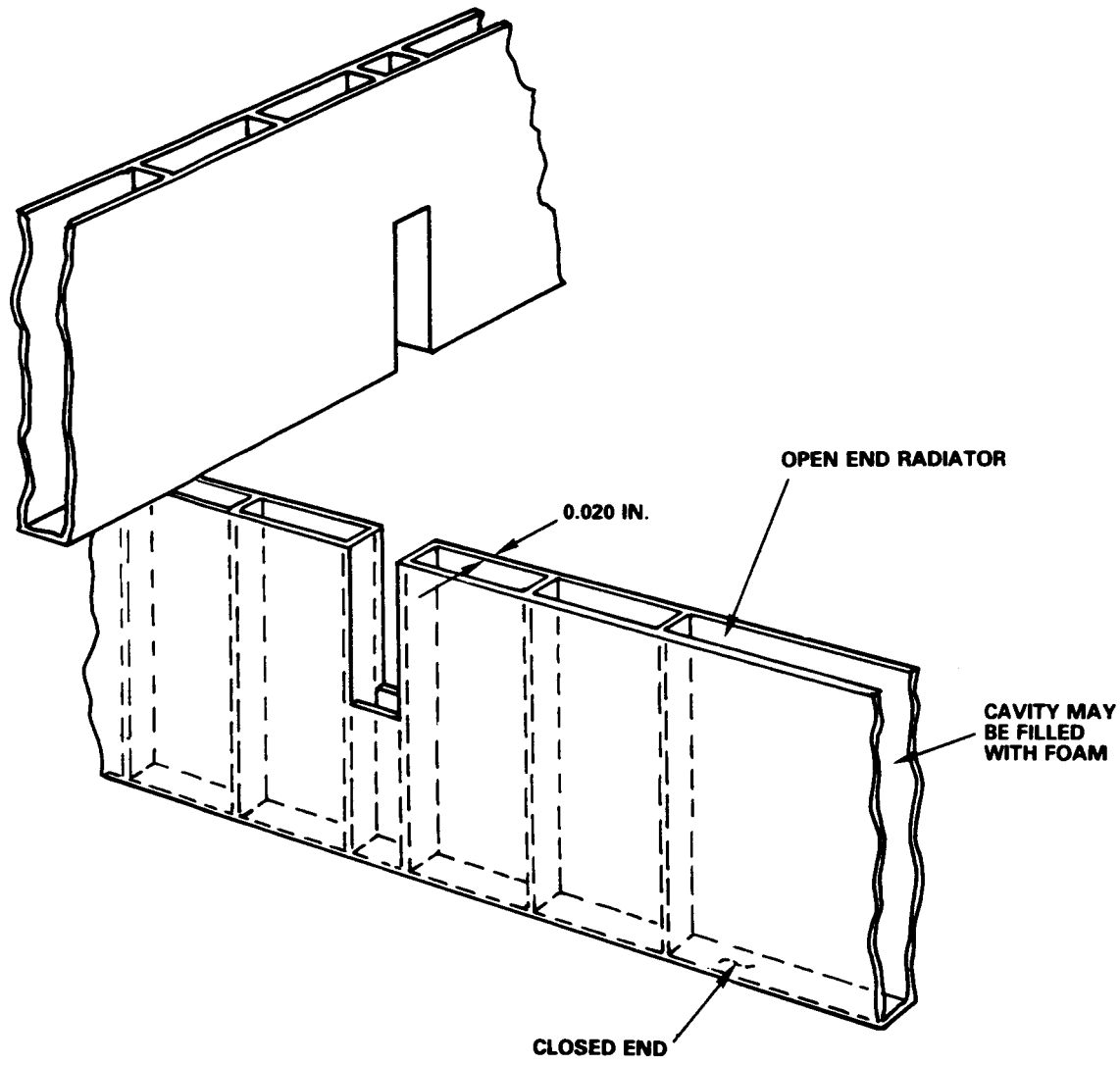


Figure II-10 – L-Band Lattice Design

c. Array Bonding Procedure

To bond the primary divider to the secondary dividers, the radiators and secondary dividers were laid up in the box and the primary divider laid in place. Faceplates were used as tooling jigs at the top and bottom of the box to align the radiators (Figure II-15).

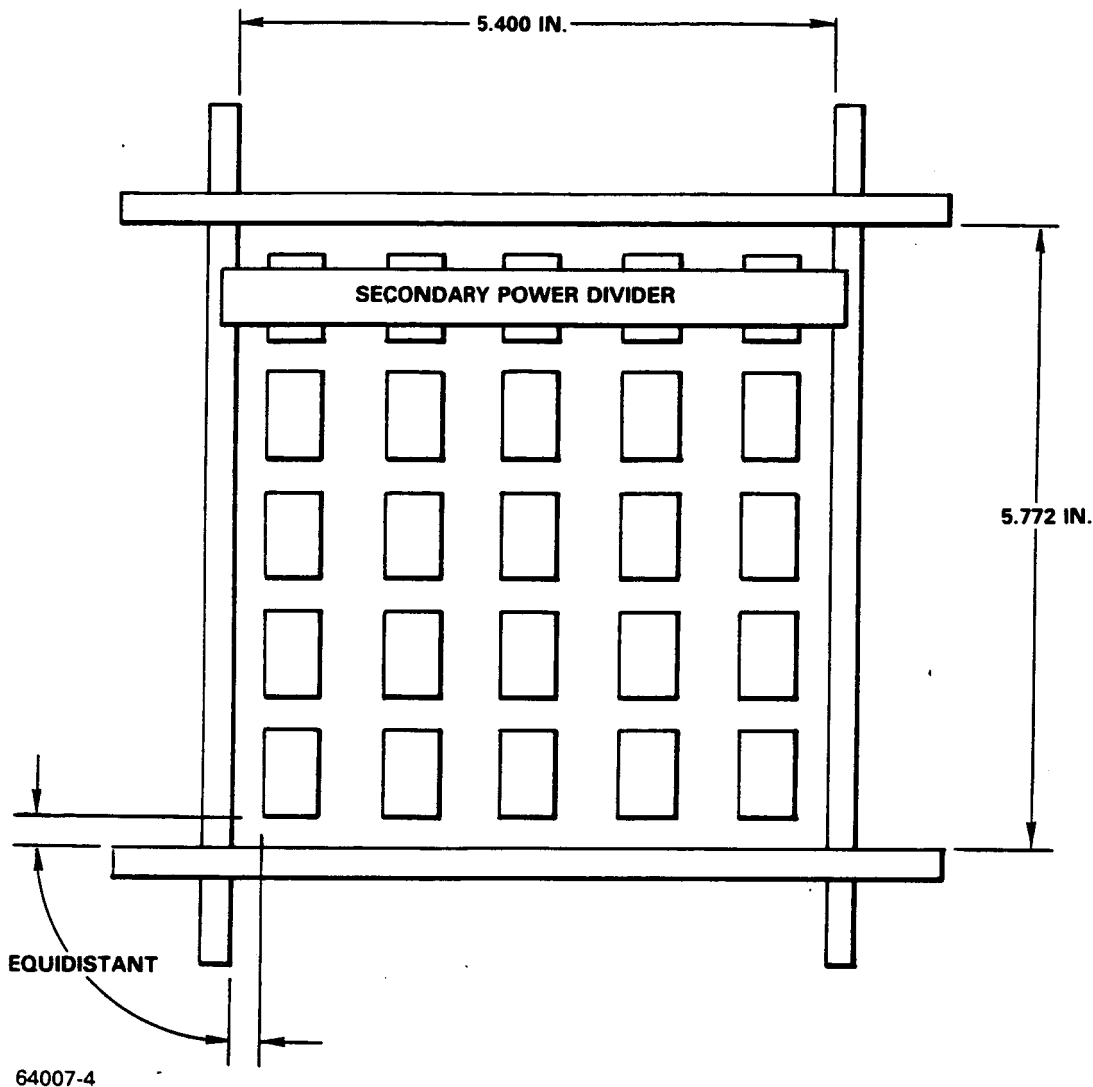
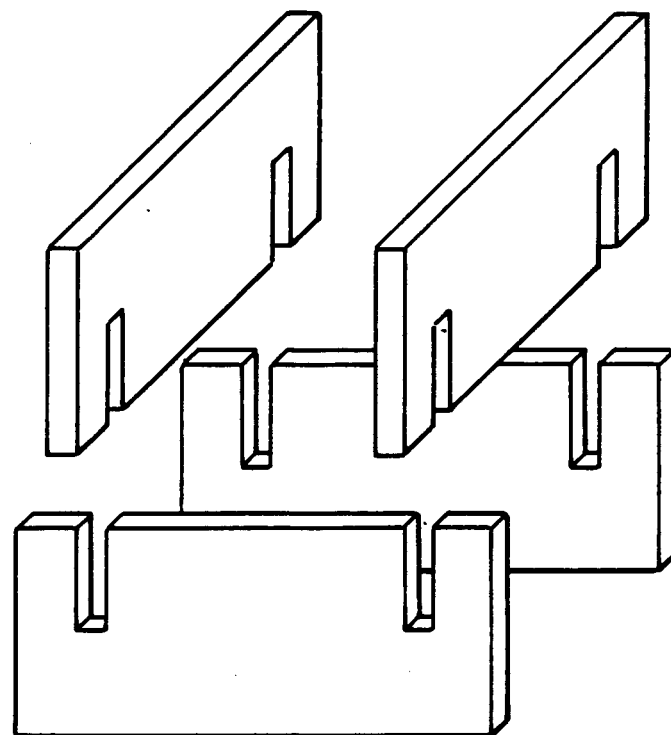


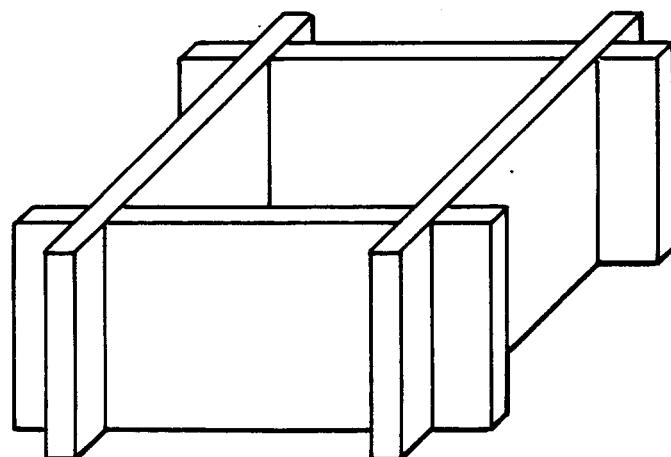
Figure II-11 - L-Band Box Layout

Fillets of 83C adhesive were applied with a syringe on three sides and allowed to set up (Figure II-16). Then the primary and secondary divider assembly was removed from the radiators and box, turned over, and 83C adhesive applied to the fourth side (Figure II-17).

Both applications of glue were very messy, so fillets were dressed with the radius of a no. 30 drill bit (Figure II-18). Then, the excess was removed with swabs and solvent. To bond the secondary power dividers to the radiators, power dividers, radiators and faceplates were again laid up in box. Secondary power dividers were tacked



INSIDE DIAMETER = 5.400 x 5.772 IN.



64007-5

Figure II-12 – L-Band Box Construction

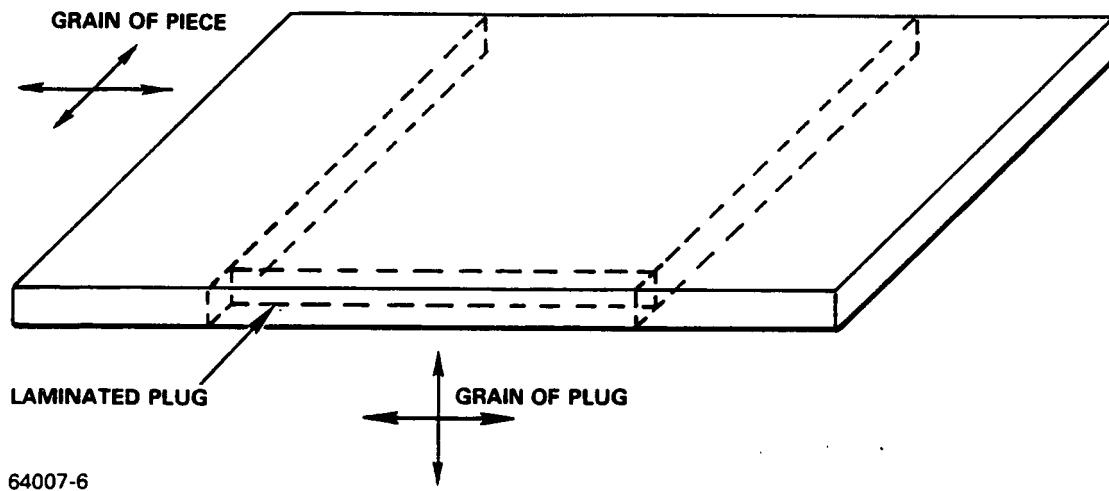
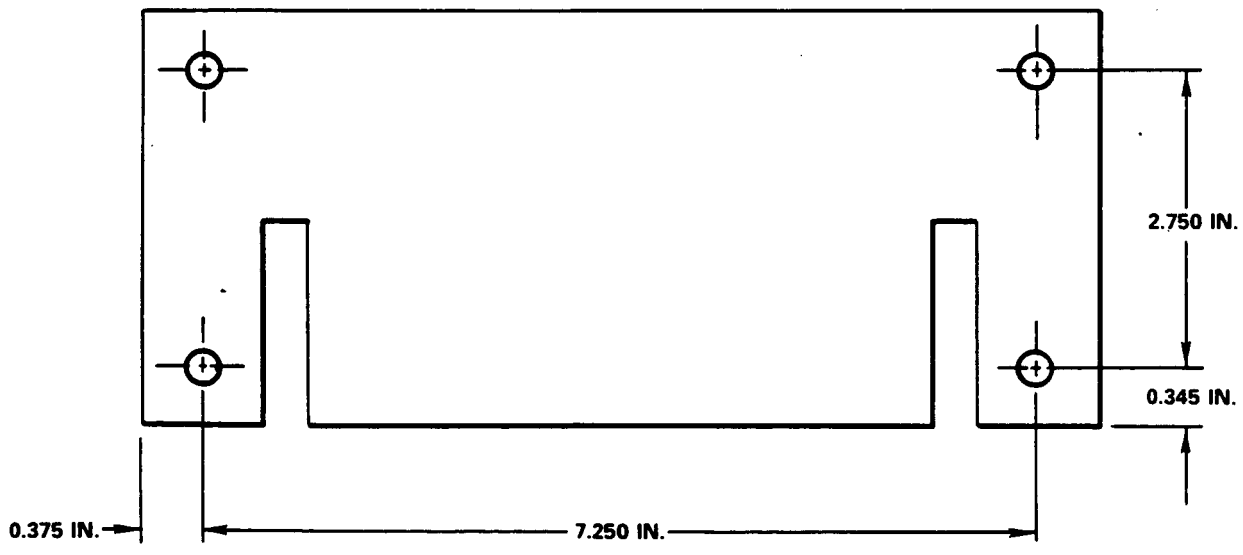
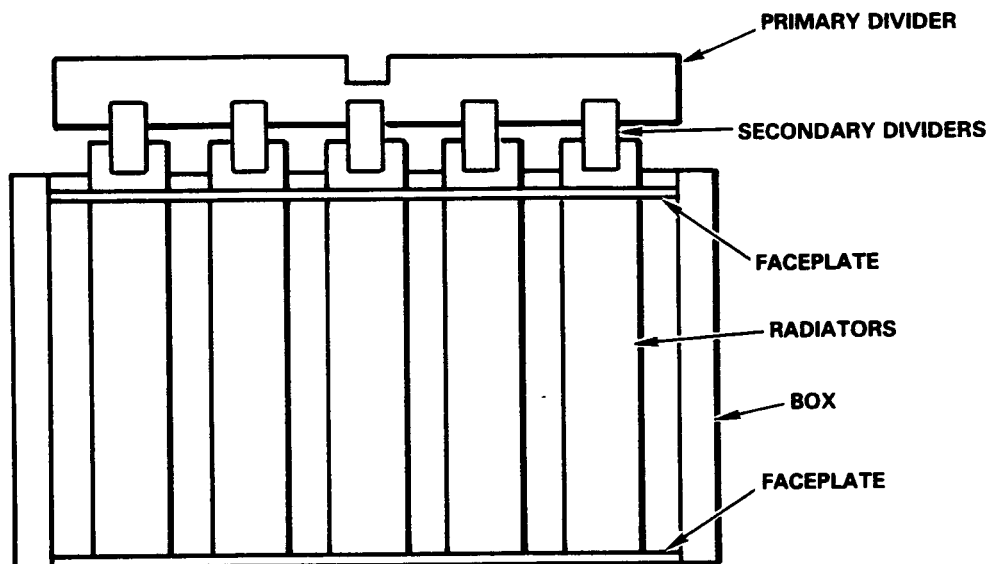


Figure II-13 — L-Band Radiator Mockup



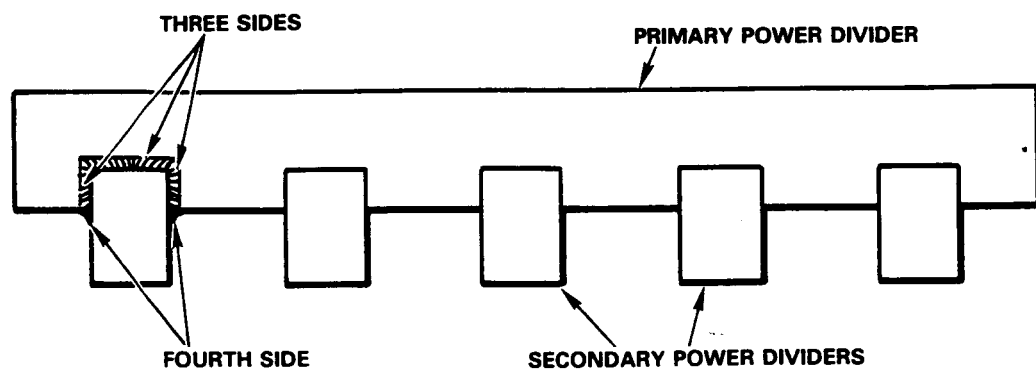
64007-7

Figure II-14 — Mounting Holes



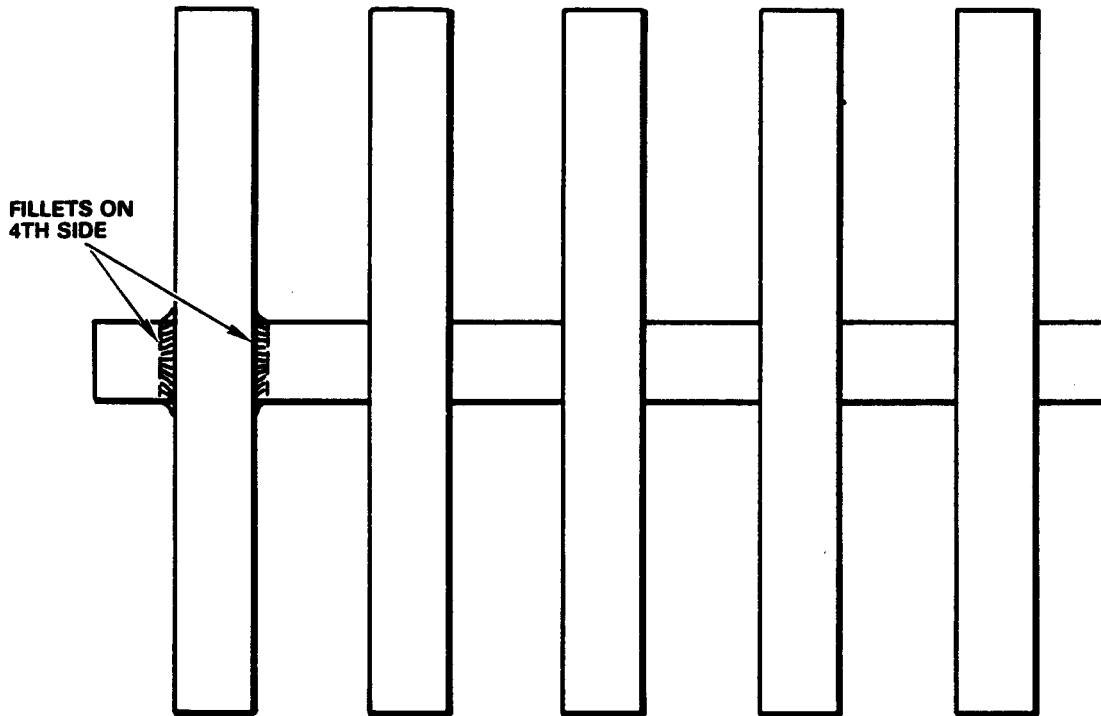
64007-8

Figure II-15 – Radiator Alignment



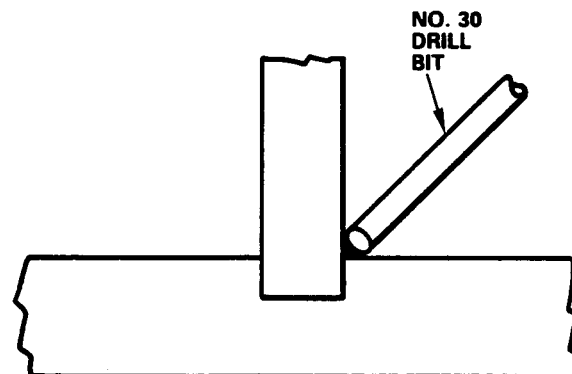
64007-9

Figure II-16 – Power Divider Bonding (Three Sides)



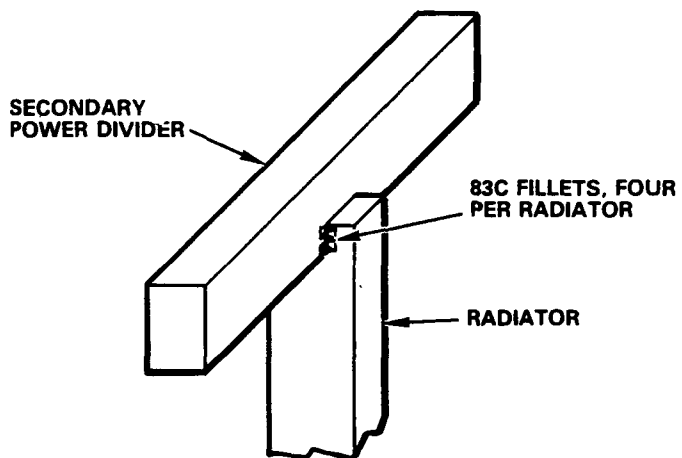
64007-10

Figure II-17 – Power Divider Bonding (Fourth Side)



64007-11

Figure II-18 – Fillet Radius



64007-12

Figure II-19 – Radiator Tack

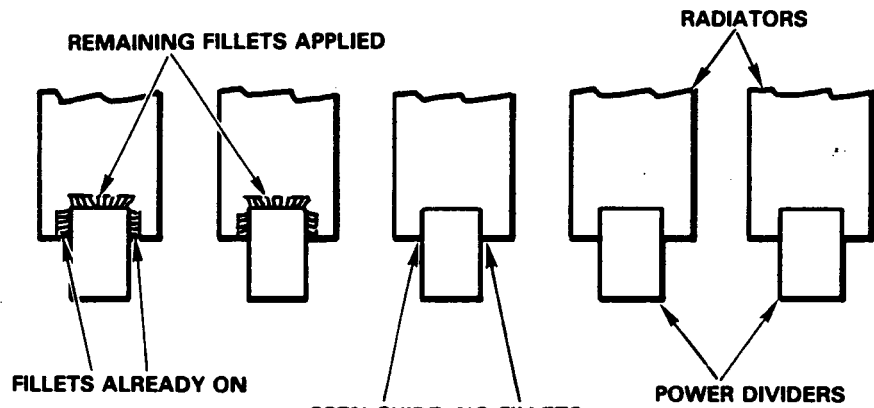
to radiators with four vertical fillets laid in with a syringe (Figure II-19) and allowed to cure. Fillets were kept neat by cleaning the excess off the tip between applications.

Then, the radiator and power divider assembly was pulled from box, turned over, and the remaining fillets applied with the syringe (Figure II-20).

To bond the radiators to the faceplate, the faceplate was secured to flat aluminum plate with lacing cord, and the power divider/radiator assembly tied into place (Figure II-21). Ecco Bond 83C fillets were applied at the inside junctions and allowed to cure.

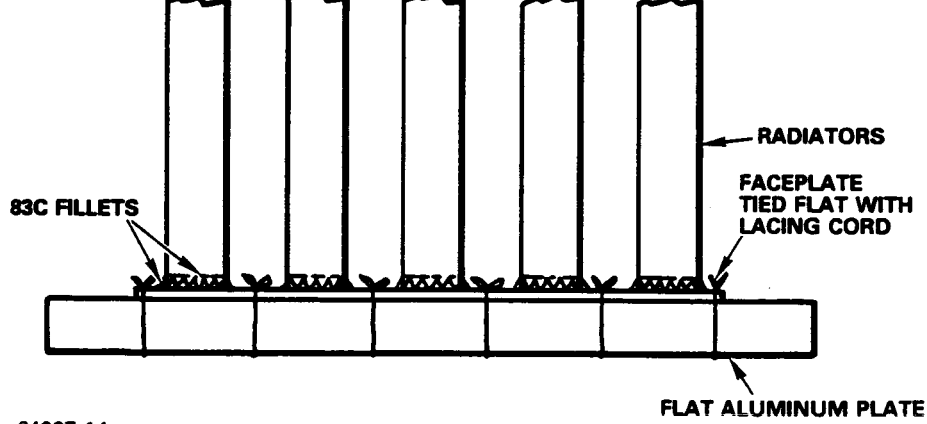
Then the assembly was turned over and 83C adhesive applied to the outer junction of the radiators and the faceplate (Figure II-22). Excess adhesive was removed. To bond the X-band array to the L-band box, the X-band array assembly was tacked to the box with EA934 adhesive (Figure II-23).

The inside of the faceplate was glued to the box using a syringe with an extended needle to reach inside (Figure II-24). The outside crack was filled with 83C adhesive and the excess removed.



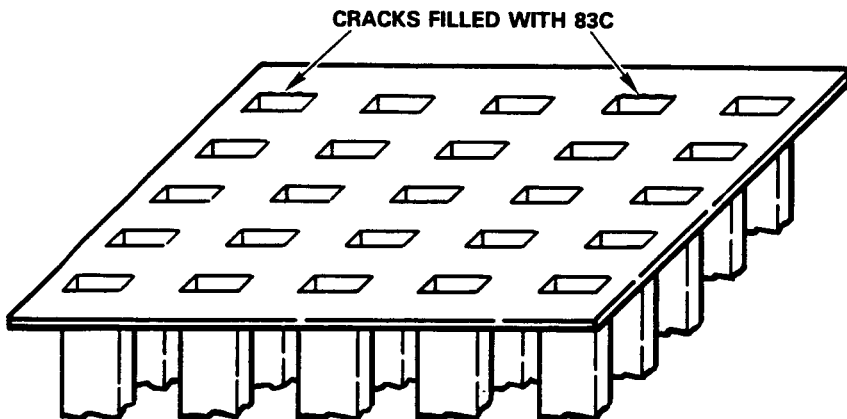
64007-13

Figure II-20 – Radiator Bonding



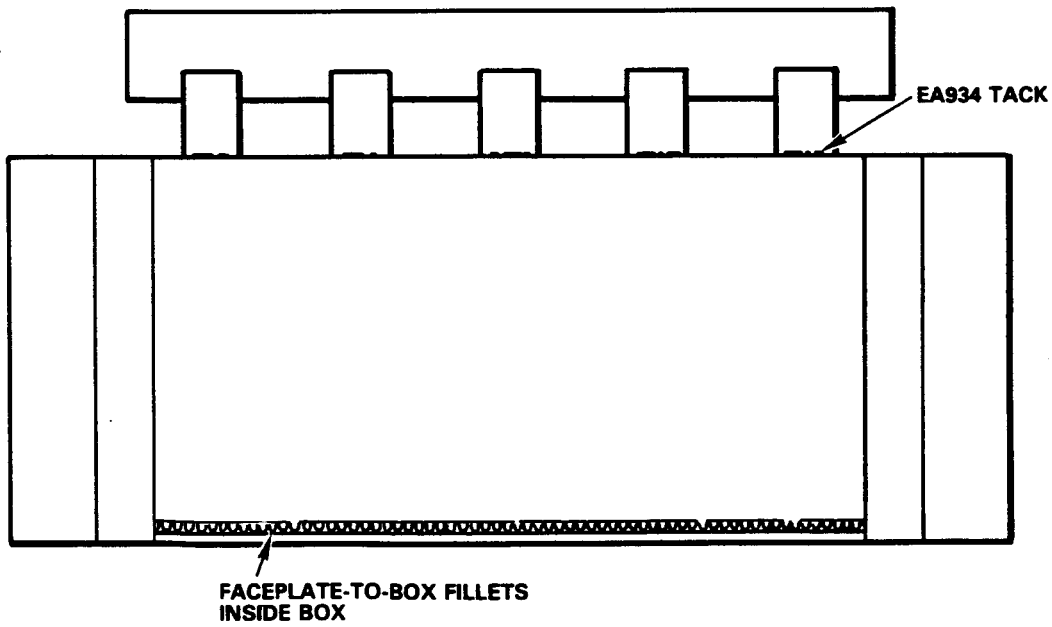
64007-14

Figure II-21 – Faceplate Bonding (Inside Junctions)



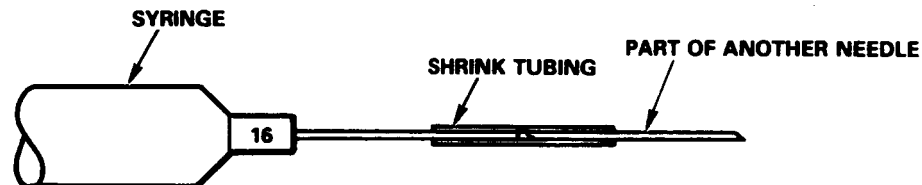
64007-15

Figure II-22 – Faceplate Bonding (Outer Junction)



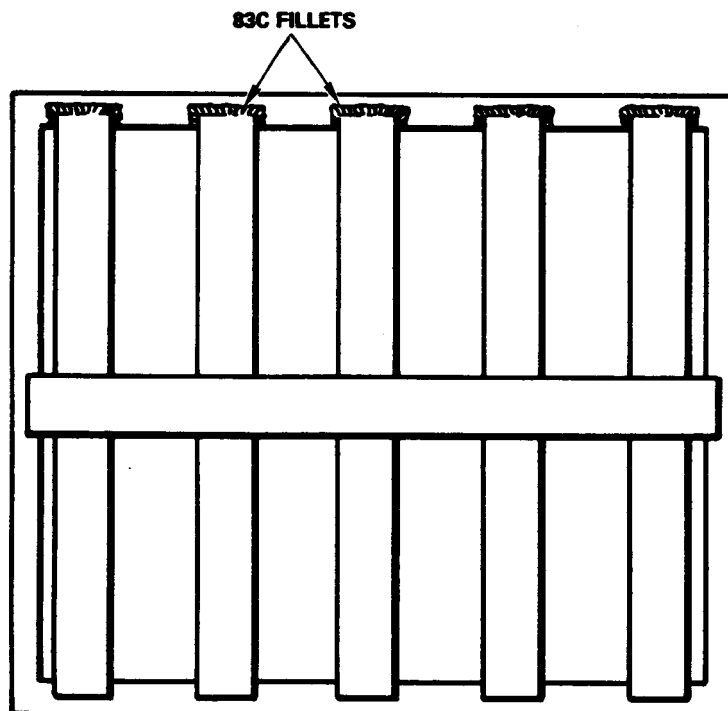
64007-16

Figure II-23 – Array Support Bonds



64007-17

Figure II-24 — Syringe Extension



64007-18

Figure II-25 — Array Support Bonds

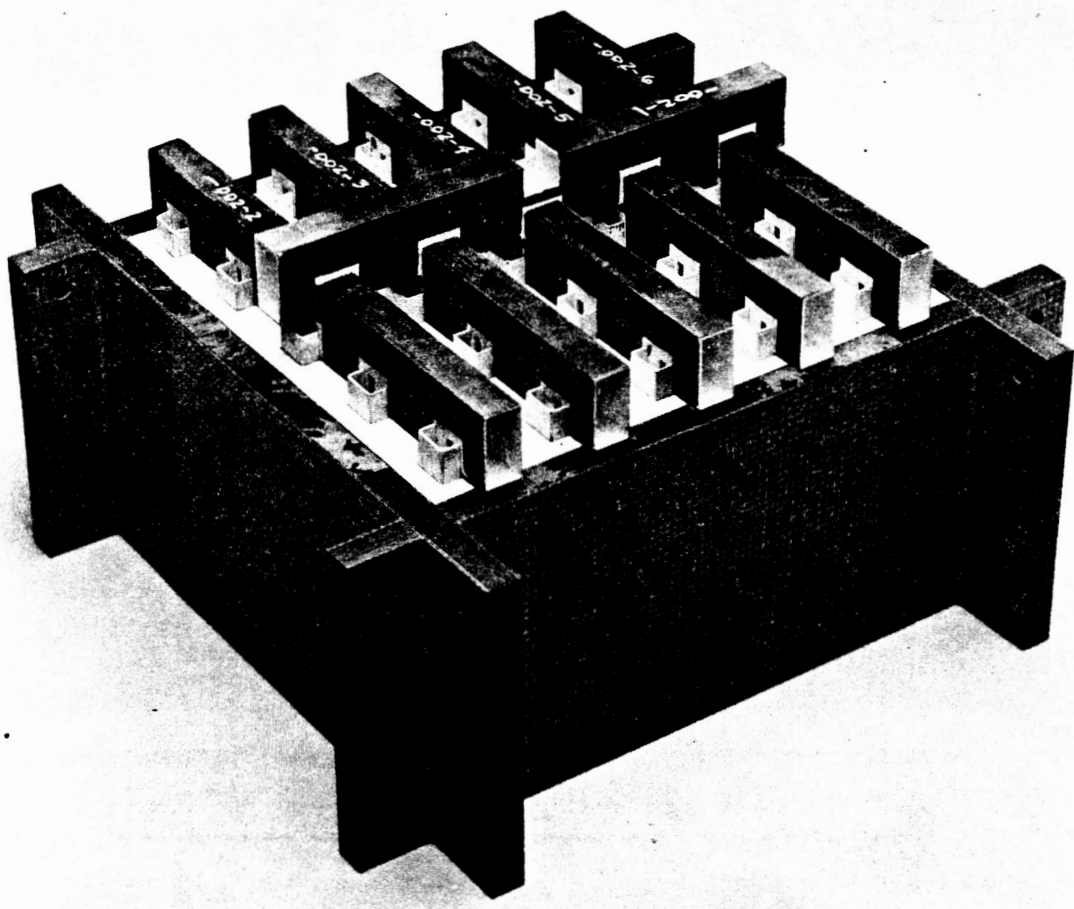
ORIGINAL PAGE IS  
OF POOR QUALITY

Fillets of 83C adhesive were run around the ends of the secondary power dividers where they contacted the box (Figure II-25).

d. Conclusion

The 5 x 5 array sits true and square and has a neat appearance. The syringe technique of applying the 83C adhesive works well if care and patience are exercised to clean the syringe tip after each bead is laid down and to remove the excess glue spillover.

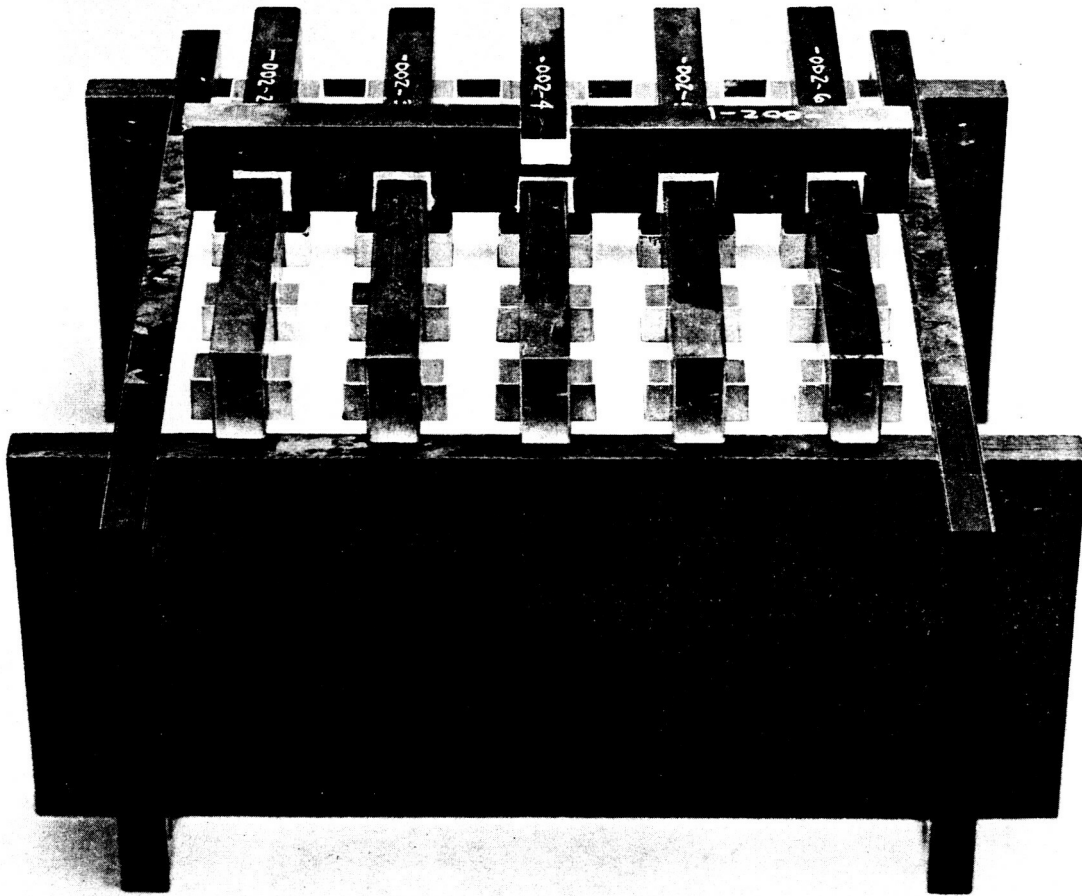
The permanent insertion of a second faceplate immediately below the secondary power dividers was considered during assembly. The faceplate was used as tooling in



G851010 01

Figure II-26 – Faceplate Supported Feed Option (Sheet 1 of 2)

this position during assembly (Figure II-15). Faceplates would close both ends of the L-band box as seen in Figure II-26 (2 sheets). This configuration would strengthen the feed end of the radiator array and eliminate the requirement to bond the power dividers to the L-band box. This configuration would be rugged, neat in appearance, and self tooling. Disadvantages include loss of access to the box interior for bonding and inspection, and increased weight.



G851010 02

Figure II-26 – Faceplate Supported Feed Option (Sheet 2 of 2)

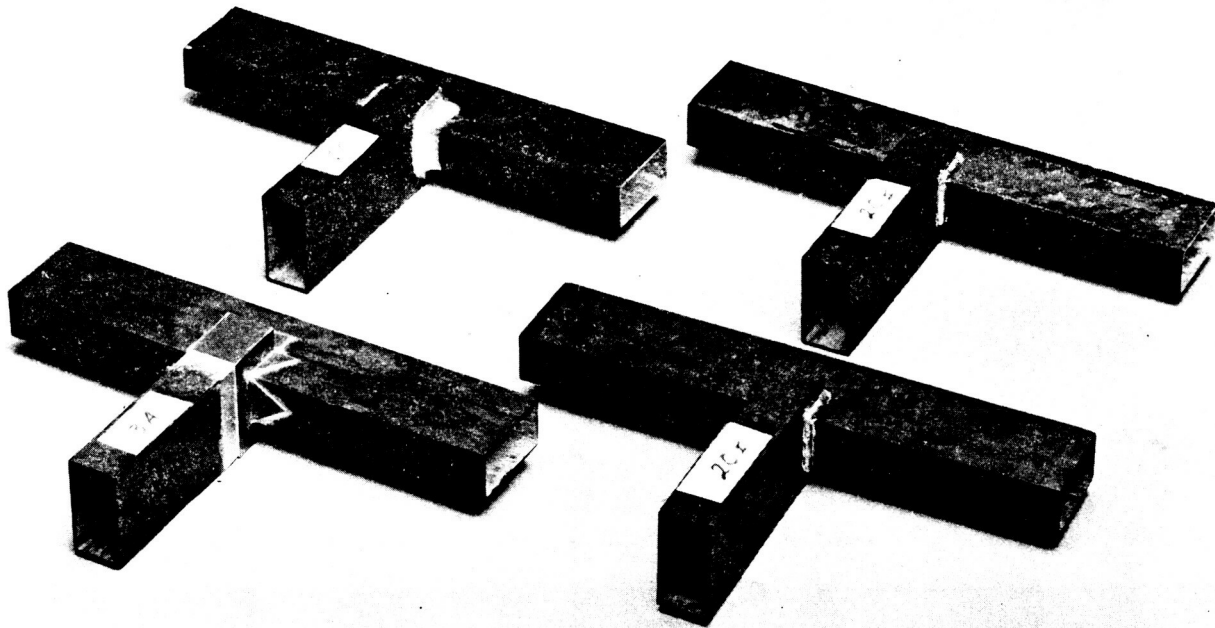
THE ORIGINAL PAGE IS  
OF POOR QUALITY

It was decided to assemble the array with a single faceplate and to environmentally test this, the weakest of the two configurations. The second faceplate is a good option should the single faceplate prove unsatisfactory.

## 5. ENVIRONMENTAL TESTING

### a. Test Results

Three environmental tests were performed to prove the mechanical integrity of the 5 x 5 waveguide array. Two temperature cycle tests were run on waveguide joint specimens. Random vibration and sinusoidal resonance search tests were conducted on the array.



G880213 37

Figure II-27 – Temperature-Cycled Specimens

Temperature cycling was not performed on the 5 x 5 waveguide array because of thermal expansion differences between the L-band box structure and the X-band array. Instead, four X-band waveguide joint specimens (Figure II-27) produced during the joint configuration development were used and the results correlated to the X-band array by similarity. Two of the joints were identical to the 25 syringe fillet joints on the array radiators. Another was a wider fillet similar to the five joints between the primary and secondary power dividers, and the fourth was a bracket joint. The temperature was cycled between -90 deg F and +160 deg F twice per the summary in Table II-4. The specimens were visually inspected after both cycles. No damage was found to any of the four specimens. The equipment listed in Table II-5 was used to conduct the test.

The 5 x 5 array was subjected to sinusoidal resonance search and random vibration in three axes. The array was mounted to the vibration table through 4 of the 16 available mounting holes in the L-band box structure. Response was monitored with two accelerometers positioned on the power divider waveguides per the sketch in Figure II-28. At each axis orientation, the array was run through a low-level resonance search from 20 to 2000 Hz, then subjected to 5 minutes of random vibration at 7.8 g (rms) as summarized in Table II-6. Tables II-7 through II-9 contain the results of the resonance search. Peak response points are emphasized by asterisks in the "Axis" columns. The maximum transmission factors found during the test were 49 on the secondary power divider during 909-Hz major axis vibration, and 48 on the primary power divider during 960-Hz minor axis vibration.

Random vibration comparable to space hardware acceptance testing was conducted after each resonance search. Vibration in excess of the level described in Table II-6 was performed for five minutes. Upon close visual inspection of the array, no damage can be found. The equipment used during these vibration tests is listed in Table II-10.

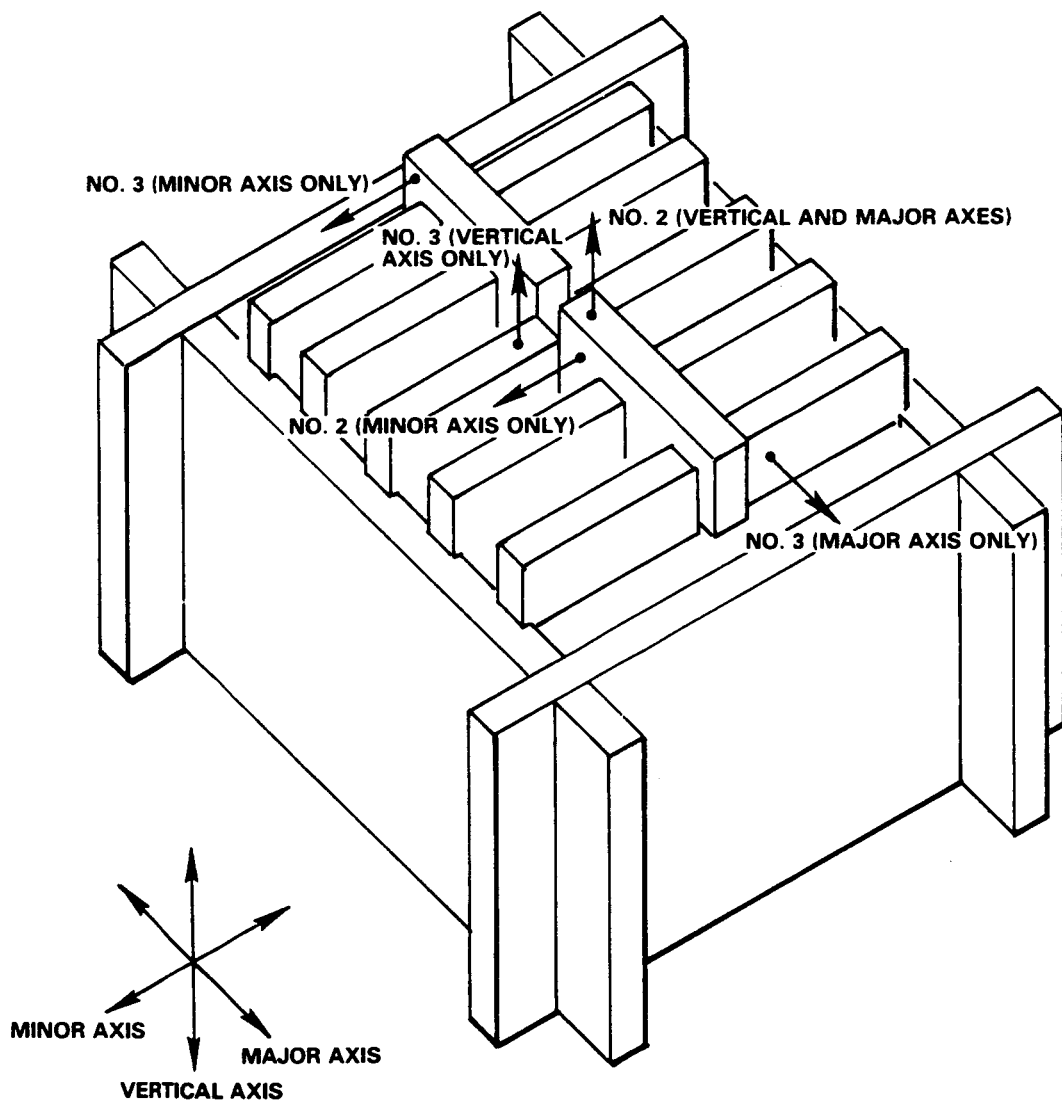
b. Conclusions

The satisfactory performance of the waveguide joints through temperature cycling can be attributed to the quasi-isotropic expansion property of the 0, 45, 135, 90, 90, 135, 45, 0 layout scheme. No flaking of the silver or cracks in the adhesive were

TABLE II-4 - TEMPERATURE CYCLE SUMMARY

TABLE II-5 - TEMPERATURE CYCLE TEST EQUIPMENT LIST

## TEST EQUIPMENT LIST



64007-19

Figure II-28 – Accelerometer Locations

found. Adhesion strength of the adhesive-to-silver and silver-to-graphite interfaces was great enough to overcome thermal stresses created by Coefficient of Thermal Expansion (CTE) mismatch of these materials.

High strength-to-mass ratio and low damping, characteristic of graphite structures, were evident by the high Qs experienced during the resonance search. Satisfactory

TABLE II-6 - VIBRATION TEST SUMMARY

RANDOM VIBRATION TEST DATA SHEET		UNIT TESTED: Mechanical Test Article, NASA Interleaved Arrays Antenna	PART NUMBER	SERIAL NUMBER
TEST PROCEDURE	Verbal Orders	TEST OPERATOR	B. Bauer (Environmental)	D. O. NUMBER 8114201
<b>REMARKS</b>				
1	10-29-85 NASA Interleaved Arrays Antenna	1206	1234	2
				A low level sinusoidal resonance search was conducted from 20 to 2000 Hz at 0.5 g.
2	10-29-85 1245	1250	2	7.8
	20-40	+12		Completed 5 minutes of random vibration at 7.8 g (RMS).
	40-500	0.06		There was no apparent mechanical damage to the test unit.
	500-2000	-1		
3	10-29-85 1348	1422	X	
				A low level sinusoidal resonance search was conducted from 20 to 2000 Hz at 0.5 g.
4	10-29-85 1439	1444	X	7.8
	20-40	+12		Completed 5 minutes of random vibration at 7.8 g (RMS).
	40-500	0.06		There was no apparent mechanical damage to the test unit.
	500-2000	-1		
5	10-29-85 1508	1542	Y	
				A low level sinusoidal resonance search was conducted from 20 to 2000 Hz at 0.5 g.
6	10-29-85 1548	1553	Y	7.8
	20-40	+12		Completed 5 minutes of random vibration at 7.8 g (RMS).
	40-500	0.06		There was no apparent mechanical damage to the test unit.
	500-2000	-1		

TABLE II-7 - VERTICAL AXIS RESONANCE SEARCH

## SECTION II

ORIGINAL PAGE IS  
OF POOR QUALITY

GERA-2758

**TABLE II-8 – MAJOR AXIS RESONANCE SEARCH**

Unit	Mech. Test Article	Part Number	Serial Number											
			Date	Axis	Freq	Input	1	2	3	4	5	6	7	8
100-29-85	MAJOR	109	0.5				0.3	2.0						
		139					0.5	3.6						
		109					0.5	3.5						
		427					2.2	1.0						
		500					0.6	3.6						
		600					0.1	1.2						
		700					0.1	1.9						
		800					0.2	4.0						
		900					2.4	2.2.5						
		*	909				2.9	2.4.5						
		1000					1.2	7.4						
		1250					3.7	5.1						
		*	1273				8.2	5.7						
		1300					5.2	7.3						
		*	1400				1.4	11.0						
		1500					0.6	4.9						
		1750					0.4	1.0						
		*	1913				0.9	6.2						
		2000	0.5				0.2	5.0						

TABLE II-9 - MINOR AXIS RESONANCE SEARCH

Unit	Mean	Test	Averages	Part Number	Serial Number	Channel Number									
						Freq	Input	1	2	3	4	5	6	7	8
10.29-PS	M.005	190	0.5					6.5	3.3						
		240						5.2	2.6						
	*	341						9.7	4.1						
	*	500						7.5	2.8						
		600						1.3	0.9						
		700						1.7	1.3						
		800						3.6	2.1						
		900						0.5	6.1						
	*	960						24.0	10.0						
		1000						14.0	5.6						
	*	1053						20.0	4.7						
		1190						17.0	3.8						
		1221						12.0	3.0						
		1300						9.2	1.8						
		1400						6.4	1.2						
		1500						4.6	1.4						
		1600						5.1	2.2						
	*	1700						12.5	4.2						
		1800						3.8	1.6						
		2000						0.9	1.4						

**TABLE II-10 – VIBRATION TEST EQUIPMENT LIST**

## TEST EQUIPMENT LIST

performance of the array through the random vibration test shows that the transmission is not excessive and the configuration strength is adequate. However, prudent design practice would take advantage of the additional support available at the radiator elements. Two easily implemented options are the insertion of the second faceplate as described in the conclusion of paragraph II. 4 and the structural attachment of the primary power divider to the L-band lattice/box. Given the low launch density of graphite array antennas, the small increase in weight would have negligible impact on cost of transport.

SECTION III – PHASED ARRAY ALTERNATIVES AND PLANS

The baseline antenna for this program is 6.9 ft high x 40.0 ft wide and contains 6 arrays: LH, LV, CH, CV, XH, AND XV.

Ground-range coverage of the system is desired to be consistent with incidence angles of 15 to 60 deg. Methods of reconfiguring the arrays from a mechanically gimballed approach to allow electronic beamsteering in the elevation (range) direction have been discussed in References 1 and 2, with emphasis on the radiator and feed parameters and the assumption that a single transmitter would be available.

An alternative is distributed amplifiers. Low-power waveform generators could be used along with low-power feed networks to distribute the signal to transmit/receive (T/R) modules at the panel, row, or element level.

Table III-1 shows the power output requirements for modules located at three different points within the antenna, based upon the specified peak power requirements.

Elevation beam scanning would be accomplished as shown in Figure III-1. A feed distribution network would connect to a phase shifter for each row, prior to power distribution through the azimuth corporate feeds.

TABLE III-1 – MODULE POWER OUTPUT REQUIREMENTS

Frequency Band	Peak Power (kW)	No. of Panels	Power per Panel (kW)	No. of Rows	Power per Row per Panel (W)	No. of Elements	Power per Element (W)
L	1.5	3	0.50	15	222	6300	1.7
C	10	3	3.33	15	222	3600	2.8
X	10	3	3.33	15	222	6300	1.6

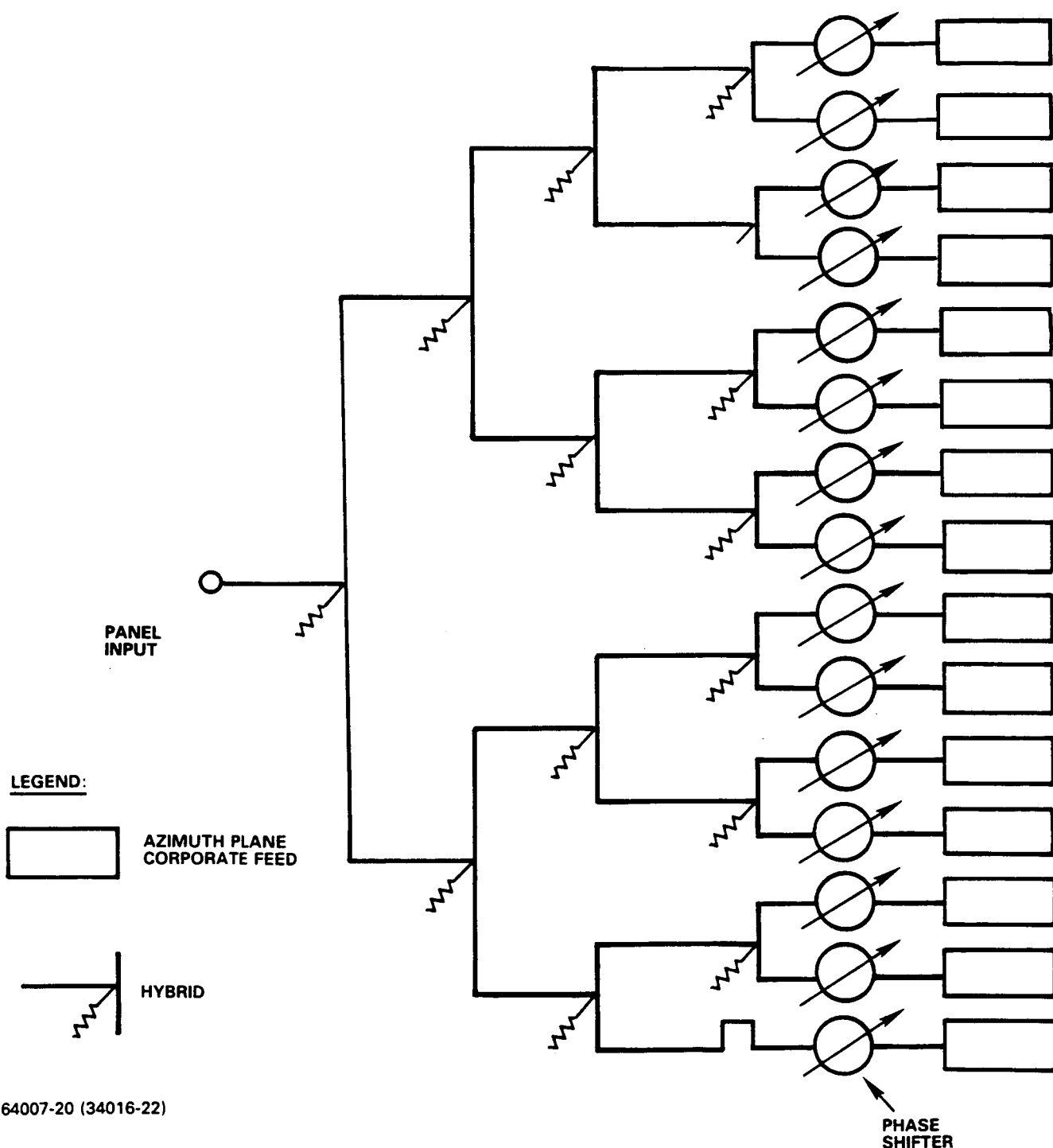


Figure III-1 – Phased Array Elevation Plane Feed Network for One Array Panel

The T/R modules could be at the panel input, combined with the phase shifter on each row, or at the azimuth corporate feed outputs to each element. As can be seen from the table, the output power per module varies dramatically with location.

A compromise location for the modules can be deduced from Figure III-2. As shown, the elements are series fed with a corporate feed, for reasons of bandwidth, beyond this point. If the C- and X-band T/R modules were located at the series feed input, the power output required per module would be reduced to 22 W, and the number of modules per panel would be 150.

For any module location at the row or element level, the phase shifters could be combined with the modules. The tradeoffs are costs and complexity of control.

A generic T/R module is shown in Figure III-3. Limiters, filters, and other components that could be required are not shown.

One approach to module realization is through the use of Gallium Arsenide (GaAs) monolithic microwave integrated circuits (MMIC). A multiple chip (phase shifter, low-noise amplifier (LNA)/switch, and power amplifier) X-band design capable of 20-W power output is probably achievable within two years at the experimental level, but questions of space-qualified units, repeatable manufacturing processes, and affordable costs would also have to be addressed.

An alternative is a traveling-wave tube (TWT) amplifier. Units with peak output powers in the 100-W to 200-W area are qualified for missile operation, are rugged, and reasonably compact. This approach would allow use of a T/R module and phase shifter per row per panel and could be designed to be removed and refurbished between shuttle flights.

Costs for MMIC T/R modules are difficult to define. Predictions for tested, working MMIC chips have ranged from \$350 to over \$1,000 in large quantities, and module costs would also have to include housings, wiring, and support parts. Modules at the element level will be difficult to justify, but may be affordable at the series feed level and may also be feasible technically.

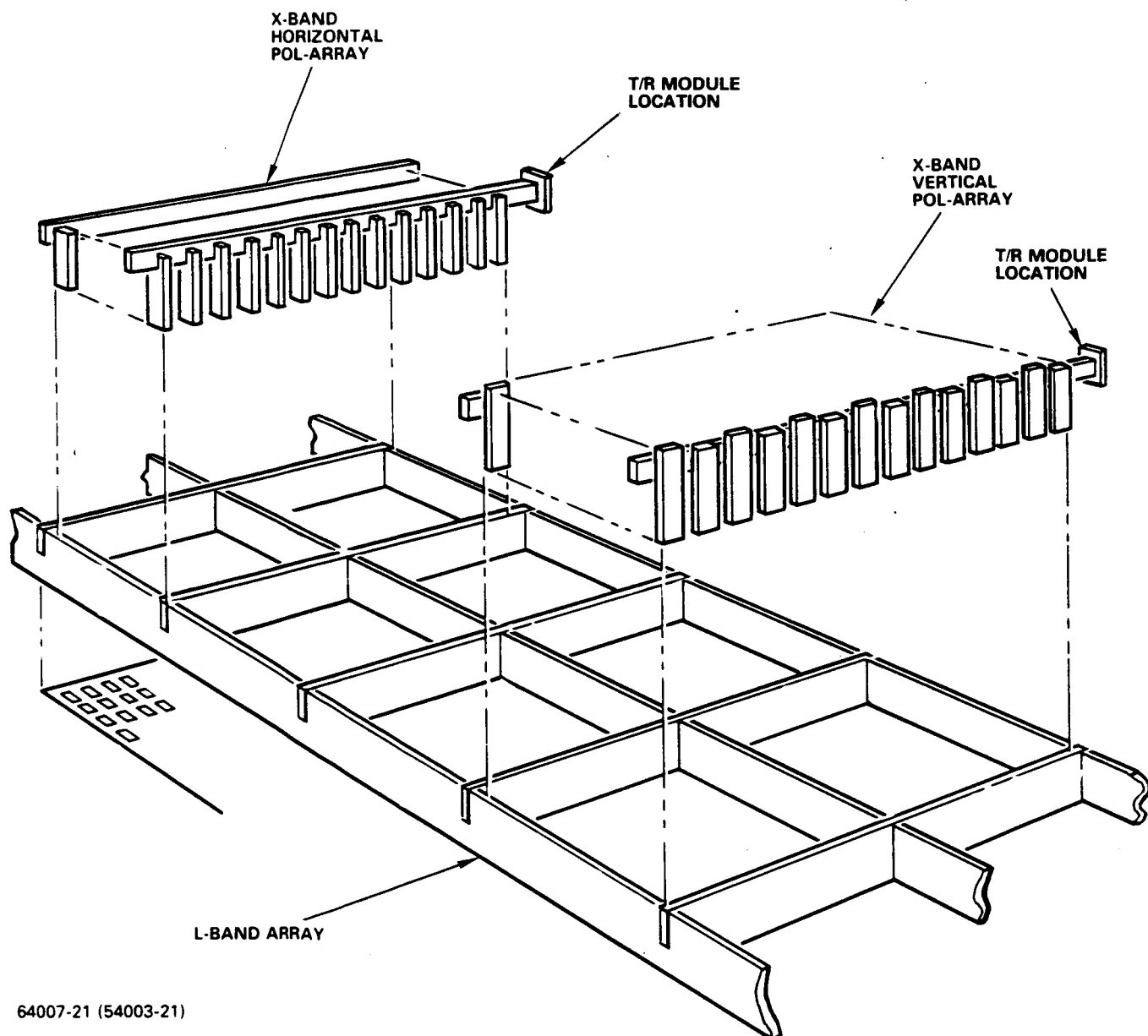
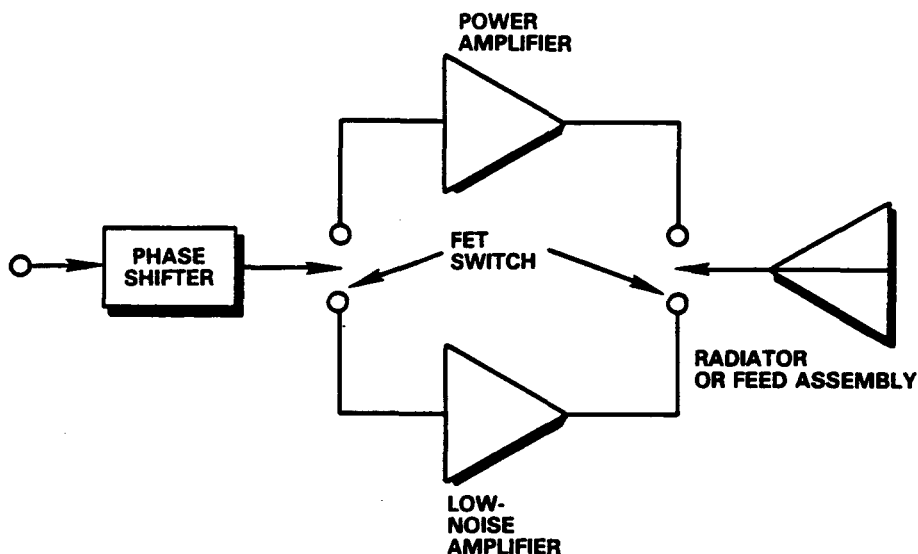


Figure III-2 – Series Feed with T/R Module



64007-22

Figure III-3 — Generic T/R Module with Phase Shifter

A possible schedule for a T/R module development is shown in Figure III-4. It is based on a TWT power amplifier bit MMIC LNA, phase shifters, and switches. This hybrid approach is considered the most feasible for near-term work, and would produce modules that could be integrated with an antenna panel for electrical, mechanical, and thermal tests.

Other equally important factors, such as thermal dissipation of the modules; distribution of prime power, control signals, and radar signals through the antenna structure; and packaging of the modules within the array structure, have not been considered in this study.

The foregoing material covers work performed as part of Phase I of this contract. Additional detailed design work was scheduled as part of Phases II and III, but was eliminated by mutual agreement between Goodyear Aerospace and NASA because of program funding limitations.

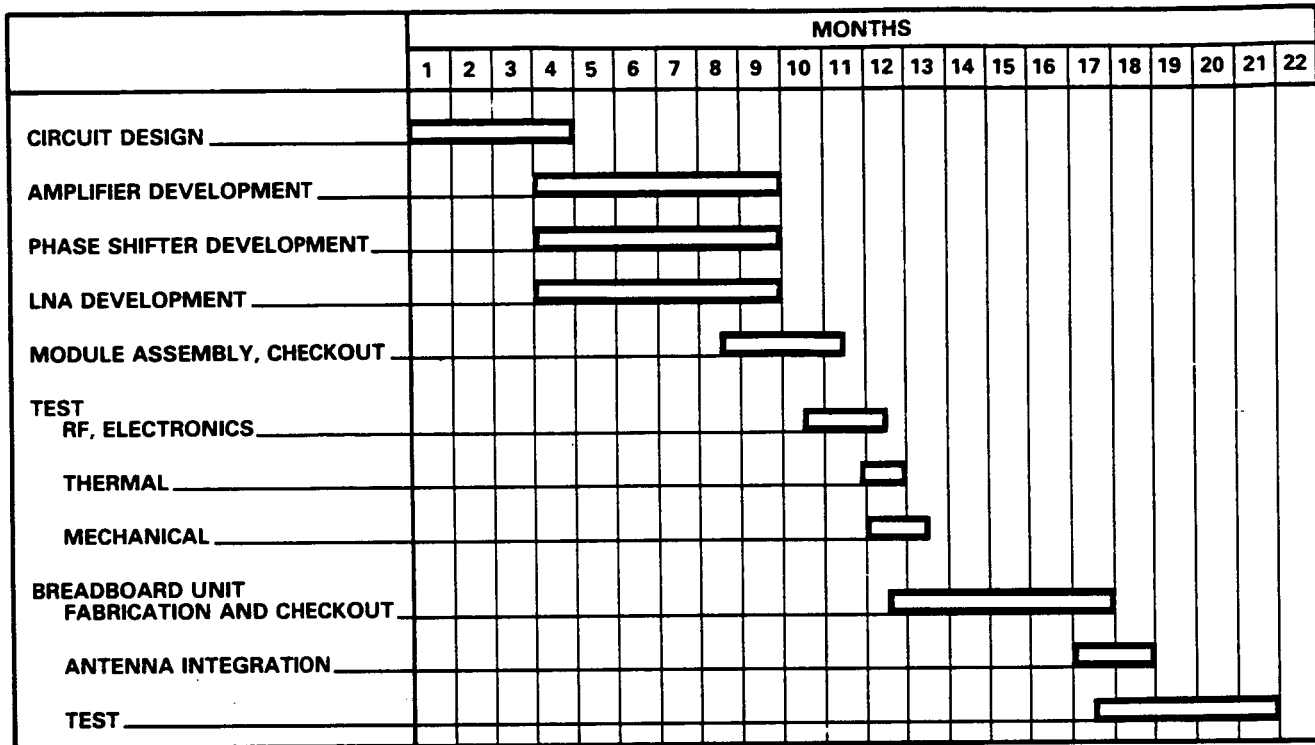


Figure III-4 – T/R Module Development Schedule